DYNAMICAL INTERACTIONS BETWEEN A MID-TROPOSPHERIC CLOSED CYCLONE, A LOW-LEVEL JET, AND CYCLOGENESIS

A Thesis

by

RICHARD LEE RITZ

Submitted to the Office of Graduate Studies of
Texas A&M University
in partial fulfillment of the requirements for the degree of

MASTER OF SCIENCE

August 1995

Major Subject: Meteorology

REPORT DOCUMENTATION PAGE

Form Approved
OMB No. 0704-0188

1. AGENCY USE ONLY *(Leave blank)*	2. REPORT DATE	3. REPORT TYPE AND DATES COVERED
	10 Sep 95	

4. TITLE AND SUBTITLE
Dynamical Interactions Between A Mid-Tropospheric Closed Cyclone, A Low=Level Jet, and Cyclogenesis

5. FUNDING NUMBERS

6. AUTHOR(S)
Richard Lee Ritz

7. PERFORMING ORGANIZATION NAME(S) AND ADDRESS(ES)
AFIT Students Attending:

Texas A&M University

8. PERFORMING ORGANIZATION REPORT NUMBER
95-093

9. SPONSORING/MONITORING AGENCY NAME(S) AND ADDRESS(ES)
DEPARTMENT OF THE AIR FORCE
AFIT/CI
2950 P STREET, BLDG 125
WRIGHT-PATTERSON AFB OH 45433-7765

10. SPONSORING/MONITORING AGENCY REPORT NUMBER

11. SUPPLEMENTARY NOTES

12a. DISTRIBUTION/AVAILABILITY STATEMENT
Approved for Public Release IAW AFR 190-1
Distribution Unlimited
BRIAN D. GAUTHIER, MSgt, USAF
Chief of Administration

12b. DISTRIBUTION CODE

13. ABSTRACT *(Maximum 200 words)*

14. SUBJECT TERMS	15. NUMBER OF PAGES
	99
	16. PRICE CODE

17. SECURITY CLASSIFICATION OF REPORT	18. SECURITY CLASSIFICATION OF THIS PAGE	19. SECURITY CLASSIFICATION OF ABSTRACT	20. LIMITATION OF ABSTRACT

ABSTRACT

Dynamical Interactions Between a Mid-Tropospheric Closed Cyclone, a Low-Level Jet, and Cyclogenesis. (August 1995)

Richard Lee Ritz, B.S.; B.S., North Carolina State University

Chair of Advisory Committee: Dr. Dušan Djurić

Output from the Eta Model was used to examine the development of a cutoff cyclone, a low-level jet (LLJ), cyclogenesis, and the interaction of these phenomena during the period 16-18 October 1994. Formation of an upper-level low followed descent of potential vorticity from the stratosphere along an upper-tropospheric front. The cutoff cyclone became established by 1200 UTC 16 October 1994, as stratospheric potential vorticity values descended to levels below 400 hPa. During this episode, a trough developed in the lee of the Rockies, and rapid cyclogenesis occurred following the movement of the upper-level low into the northern Great Plains.

To study this event, the Eta Model was chosen. The high spatial and temporal resolution of the Eta Model made it suitable for studying the development of the cutoff cyclone and the LLJ. A statistical analysis of the Eta Model results indicated that the model provided an accurate representation of the atmospheric situation.

The formation of a cutoff low followed the descent of high potential vorticity air into the middle troposphere with the cyclone cutting off from the westerly current when the potential vorticity maximum became isolated in the base of the trough. The upper-level

cyclone interacted with the low-level baroclinic zone initiating the development of a lower-level cyclone.

A LLJ developed over the central United States in association with a deepening trough in the lee of the Rockies and an upper-level jet (ULJ) streak propagating to the northeast from the southwestern United States. The LLJ was coupled to the return branch of the indirect circulation in the exit region of the ULJ; Q-vector convergence indicated that the LLJ was driven by large-scale forcing.

A schematic diagram was constructed using existing theories concerning the development of a surface cyclone, interaction with an upper-level cyclone, the LLJ and the ULJ. The rapid development of the surface cyclone was related to the interactions of the upper- and lower-level cyclonic systems and the LLJ and ULJ.

ACKNOWLEDGEMENTS

The author would like to thank Dr. Dušan Djurić for his support and guidance in the preparation of this paper. I want to thank Dr. James P. McGuirk for his advice and recommendations in leading me to a meaningful and appropriate conclusion to this research, and Mr. Robert White and Mr. Daniel Austin for their assistance in the use of department computer resources. Also, I want to thank Dr. Omer C. Jenkins for his guidance and assistance with the statistical evaluations.

Extensive support from Mr. Paul Janish at the National Severe Storms Laboratory (NSSL) made it possible to acquire the data for this research, and the staff at the United States Air Force Environmental Technical Applications Center (USAFETAC) provided library resources needed to complete this work.

TABLE OF CONTENTS

CHAPTER Page

LIST OF FIGURES

FIGURE Page

FIGURE Page

FIGURE Page

CHAPTER I

INTRODUCTION

Operational forecasters use a variety of conceptual models to determine the potential for the occurrence of particular weather phenomena. These conceptual models are based on research of various cases of a particular phenomenon. For example, forecasters use these models to predict heavy snowfalls in Colorado (Barnes and Colman 1993). Another of these models describes the eastern Pacific developmental trough (Weismueller 1984, Tollerud et al. 1991). This trough is similar to the type-B developing baroclinic wave model (Petterssen and Smebye 1971), and the California cutoff cyclone is a subset of this trough. These cyclones in combination with other factors can have a significant impact producing heavy snowfall in the Colorado Rockies.

Previous research conducted in the 1940s through the 1960s established the structure of these cyclones through observational studies, and recent research has continued to study the dynamics of these mid-tropospheric features through the use of numerical weather prediction models and the use of isentropic analysis. Increased spatial and temporal resolution of the current numerical weather prediction models, as well as a better understanding of atmospheric physical processes, has enabled the researchers to further delve into the dynamics involved in these cyclonic events.

The style is that of the *Monthly Weather Review*.

Occasionally, a low-level cyclonic circulation forms in association with these mid-tropospheric cutoff cyclones as the upper-level potential vorticity maximum moves over a lower-level baroclinic zone or a lower-level potential vorticity maximum. Associated with these lower-level cyclones is a feature known as the low-level jet (LLJ). This feature is of interest to forecasters in the central United States where the LLJ serves as a conveyor of low-level moisture and is often found in association with outbreaks of severe convection. Many studies have been conducted into the boundary layer processes driving these LLJs, but only recently has there been an interest in the synoptic features associated with these strong low-level winds.

A. Objectives

The goal of this research was to establish a dynamical relationship between a cutoff cyclone, a LLJ, and a surface cyclone for a case in the western and central United States. The first objective of this research was to describe the horizontal and vertical processes that led to the development and evolution of this mid-tropospheric closed cyclonic event and how its interaction with a lower-level potential vorticity maximum was associated with lower-level cyclone development. This cyclonic system was examined by using output from the Eta Model, as well as radiosonde data, to describe processes occurring in the development and evolution of this cutoff cyclone and surface cyclone. The second objective was to describe the development of the LLJ during the lower-level cyclonic event.

Questions may be asked: How did the LLJ develop? What were the forcing mechanisms? The third objective was to show the interaction of the LLJ and the upper-level jet (ULJ). How were these two jets related in the development of a surface cyclone? This thesis will attempt to give answers to these questions.

B. Procedures

An upper-level cyclone moved into the western United States and cut off from the westerly current. The cyclone remained nearly stationary for 24 hours and then moved off to the east-northeast. At the time the upper-level cyclone was moving out of the western United States into the Central Plains, surface cyclogenesis commenced over the Central Plains with an associated LLJ. The surface cyclone deepened rapidly becoming vertically aligned with the upper-level cyclone.

To accomplish the goal of this study, three objectives were stated. The first objective was accomplished by following these procedures:

1. A statistical analysis of the model output was performed to verify the reliability of the Eta model initialization data and forecast data to the radiosonde data.

2. Vertical sections in time and space for the radiosonde data and the model soundings for this research were constructed to examine mid-tropospheric processes which may have had an impact on the development of the cutoff cyclone.

3. Plots of potential vorticity on isentropic surfaces were performed to

evaluate the evolution of the upper-level cyclone and its interaction with the lower tropospheric baroclinic zone in the development of the lower tropospheric low.

The second objective was accomplished by following these steps:

4. The forcing mechanisms for the LLJ were identified through the calculation of the geostrophic, ageostrophic, and isallobaric components of the flow.

5. Q-vector analysis (Hoskins et al. 1978) was used to determine the vertical and ageostrophic motions involved with the LLJ and synoptic scale features involved in this case.

The third objective was accomplished by following these steps:

6. Vertical sections through the ULJ and LLJ were made to analyze the vertical structure of the circulation.

7. Vertical sections were made through the upper-level cyclone and lower-level cyclone to analyze the interaction between these two circulations.

8. A conceptual model was devised to show the dynamical interaction between the upper-level low and its associated jet and the surface low and its associated LLJ.

CHAPTER II

SURVEY OF LITERATURE

Palmén and Newton (1969) give a comprehensive review of the research conducted in the area of upper-level cyclones stating that these cyclones have been called by various names: high-level cyclone, cold vortex, and cutoff low. All of these names describe a system which has the following characteristics:

(1) Upper cyclones are associated with a dome-shaped region of cold air in the troposphere

(2) Lows at 500 hPa have a cold center

(3) The tropopause dips down over the cold dome, and

(4) This type of vortex has a warm core in the lower stratosphere.

Palmén (1949) indicates that there are regions where the formation of cutoff cyclones is favored. He observed that cutoff cyclone formation often occurs in the western United States and in southern Europe.

Knowing that there are regions favored for development leads to the question of how these systems develop. A cutoff cyclone can form in the final stage of cyclogenesis when the occlusion process reaches a climax, or a cutoff low can form as a jet streak in a

northwesterly flow propagates toward the base of a broad diffluent trough. During the development and evolution of these cyclones, a fold in the tropopause is observed to occur over the cyclone. Later researchers studied this fold and its impact on the development of these systems.

The funnel-like structure observed by Palmén led Kleinschmidt (1950a,b) to theorize that the cyclonic circulation of a cutoff low is induced by the anomalous distribution of stratospheric air high in potential vorticity above the circulation center. This leads to the concept of a tropopause fold which is defined by Reed (1955) and Reed and Danielsen (1959) as the extrusion of stratospheric air within a normal tropopause level to the middle and lower troposphere. This work provides the basis for further research into the role of potential vorticity and its role in the formation and maintenance of cutoff cyclones. Palmén and Newton (1969) review the work performed in the 1950's and 1960's. Their review shows that the understanding of the structure and the dynamics of a cutoff cyclone comes from the application of the concept of the tropopause fold and the role potential vorticity plays in the formation of a cutoff cyclone.

Recent research has tapped the earlier works of Rossby and Kleinschmidt. Hoskins et al. (1985) extensively review these earlier researchers' works and provide a thorough discussion of the use of the isentropic coordinate system and the invertibility principle described by Kleinschmidt (1950a,b). They note that the analysis of maps of isentropic potential vorticity is beneficial in providing the basis for comparisons between atmospheric models and the observations of the atmosphere. At levels away from the surface of the

earth, the isobaric analyses look similar to the isentropic charts. This is clearly shown through the examination of a cutoff cyclone using isentropic potential vorticity charts to show the evolution of this cyclone. A comparison to the 500 hPa chart for the same time frame shows similar structures but the 500 hPa chart shows it in a highly smoothed manner.

Thorpe (1985, 1986) worked with the invertibility principle for isentropic potential vorticity for the balanced flow structure of atmospheric disturbances on the synoptic scale. He states from his research that the observational studies of cutoff cyclones by Palmén (1949), Peltonen (1963) and Shapiro (1978) have many structures which can be accounted for by the invertibility principle. Prior to the formation of a cutoff low, a strand, or as Palmén and Newton (1969) state, 'an umbilical cord' of potential vorticity is noted connecting the cyclone with the stratospheric source of potential vorticity.

These studies, as well as recent studies, point to the important role played by potential vorticity in the process of cutoff cyclogenesis. Bell and Bosart (1993) studied the formation of a cutoff cyclone over the eastern United States during the Genesis of Atlantic Lows Experiment (GALE). They state from their results that the formation of a cutoff cyclone results from the descent of stratospheric air in a northwesterly flow, and that the confinement or isolation of this center of high potential vorticity within the base of the diffluent long wave trough is the signal for the formation of a cutoff cyclone to occur. They also observe the lack of strong baroclinic development in the lower troposphere even while a vigorous upper tropospheric event is occurring above the region. This is consistent with the general consensus that a full-scale development throughout the atmosphere is most

often seen when an intensifying short wave trough moves into a region of a well defined lower tropospheric baroclinic zone (Petterssen 1956). The structure of the closed cyclone observed by Bell and Bosart (1993) is consistent with the idealized closed cyclonic circulation center described by the invertibility principle of potential vorticity (Thorpe 1985). Thorpe (1986) states that it is apparent that the proper representation of the troposphere/tropopause in numerical weather prediction models is needed to accurately describe the synoptic flow. He states that an increase in the vertical resolution of the current weather prediction models near the tropopause or the use of isentropic coordinates may improve the description of the tropopause.

Bell and Bosart (1993) also studied the contributions by upper- and lower-tropospheric forcing in the formation of the cutoff cyclone from the perspective of the quasi-geostrophic potential vorticity equation. Their results indicate that the stratospheric air advected by the northwesterly flow is a contributing factor in the significant height falls upstream of and within the long wave trough. Large cyclonic vorticity increases in the middle troposphere are observed as the tropopause descends to levels below 500 hPa. The closed circulation continues to intensify as the jet streak becomes more centered in the base of the trough with a further increase in the potential vorticity and temperature above the cutoff cyclone at levels within the extruded tropopause.

The jet streak which plays an important role in the development and evolution of a cutoff cyclone is an important factor in the development of the LLJ. Blackadar (1957) studied the LLJ finding that the LLJ reaches a maximum speed at 2000 ft above the

ground, and that the flow is subgeostrophic during the day becoming supergeostrophic following establishment of the nocturnal inversion. The LLJ in general has its maximum winds at about 800 m above the surface with speeds as high as 30 m s^{-1} (Bonner 1965). A statistical analysis of the LLJ across the United States shows that there is a region of maximum occurrence extending from Texas to Nebraska (Bonner 1968).

Studying the LLJ, Wexler (1961) proposed that the primary cause for the formation of the LLJ is that the flow in the lower atmosphere is forced northward along the periphery of the Rocky Mountains where the mountains act as a barrier. This theory is analogous to the western boundary current model used to describe the flow in the oceans.

Hoecker (1963) disputes Wexler (1961) by noting that in his cases, the well-defined jet occurs with a polar anticyclone rather than from a trade wind source. Using measurements from a group of PIBAL stations, Hoecker found that when high pressure is situated to the east of the Great Plains region, a well-developed nocturnal jet forms. During the day, this jet is poorly defined.

Holton (1967) states that although the hypothesis put forth by Wexler provides a mechanism for the generation of the weak LLJ observed during the daytime, it cannot explain the diurnal variation. Holton says that the nocturnal variation in the frictional forces alone cannot explain the amplitude and structure of the LLJ. The variation of eddy viscosity in time and space must be included in the argument to account of the structure and phase of the LLJ.

The previous research focused on the LLJ which occurs in the planetary boundary

layer, but recently there has been an interest in the LLJ and its relationship to synoptic-scale features. In a case study involving an outbreak of severe weather over Ohio (10-11 May 1973), Uccellini and Johnson (1979) presented evidence to support the coupling of the upper-tropospheric jet and the LLJ. This is accomplished thorough a two-layer mass adjustment in the exit region of the upper-level jet streak. The LLJ is observed to develop as a result of the pressure gradient induced by the redistribution of mass aloft and the increased isallobaric wind component in the lower troposphere. Uccellini (1980) describes this LLJ as a Type 1 LLJ. This jet forms as a result of synoptic-scale forcing and exhibits a well organized structure during the afternoon. This jet also shows a maximum in wind speed during the morning hours.

Uccellini (1980) notes that most of the previous research concerning the LLJ has not related this feature to synoptic-scale features. He examined 15 cases of LLJs which formed over the central United States. In 12 of the 15 cases he reviewed, a LLJ developed in response to lee cyclogenesis or lee-side troughing in the area of the Rocky Mountains or in response to a jet streak in the upper troposphere.

Djurić and Damiani (1980) examined the formation of a LLJ over Texas during the winter period to identify the region of development of this feature. They indicate that the formation of a LLJ generally occurs under the upper-tropospheric northwesterly flow behind the trough associated with an outbreak of cold air across the Great Plains. A short wave trough develops in the lee of the Rocky Mountains, and the pressure falls with the resulting establishment of a LLJ. The LLJ first develops in northwestern Texas and spreads

rapidly to the Gulf of Mexico.

Djurić (1981) studied the formation and evolution of a LLJ using a one-layer, one-dimensional model. He states that the pressure falls, and cyclogenesis in the lee of the Rockies initiates the development of the LLJ. Djurić and Ladwig (1983) found similar results in 20 cases of LLJ during the winter half of the year and that the development of the LLJ occurs early in the cyclogenesis phase near the eastern foothills of the Rocky Mountains. They indicate that there is a relationship between the occurrence of the LLJ and the upper-level jet streak exit region as described by Uccellini and Johnson (1979) and Uccellini (1980). But Djurić and Ladwig indicate that there are cases where the LLJ occurs in the entrance region of the jet streak. The simultaneous development of the LLJ and a surface cyclone support the theory that the pressure fall is the mechanism responsible for the LLJ (Djurić and Ladwig 1983).

Djurić and Ladwig (1983) and Uccellini et al. (1987) show that a LLJ is often observed accompanying cyclogenesis. But deep tropospheric cyclogenesis in association with a cutoff cyclone does not always occur. Hoskins et al. (1985) indicate that the potential vorticity source in the stratosphere can act to increase the cyclonic circulation in the low-levels. They state that since the cutoff cyclone is a region of cyclonic potential vorticity, as it arrives over a pre-existing baroclinic zone, low-level thermal advection will result in the development of a warm anomaly ahead of the upper-level system. This will enhance the warm advection already in place inducing a cyclonic circulation. The result is that the low-level circulation adds to the upper-level circulation resulting in an intense

cyclone just ahead of the upper-level isentropic potential vorticity anomaly. The upper- and lower-level maxima tend to become phase-locked resulting in a mutual intensification of each feature.

The processes leading to the development and evolution of a cutoff cyclone are well documented (e.g., Palmén and Newton 1969, Hoskins et al. 1985). Formation of the cutoff cyclone occurs when a surface cyclone occludes or a when a jet streak in a northwesterly flow propagates into the base of a diffluent trough. The forces responsible for the development of the LLJ are also well documented (e.g., Hoecker 1963, Djurić 1981). The LLJ forms in response to boundary layer forces or in response to synoptic-scale forcing. Where boundary layer forcing is occurring, the LLJ forms as a result of diurnal variation in the frictional forces in the boundary layer (Blackadar 1957) with the formation of a nocturnal radiational inversion. Where synoptic-scale forcing is occurring, the LLJ may form in response to low-level cyclogenesis or an upper-tropospheric jet streak.

There has been little research concerning the interaction between an upper-level cyclone and its associated jet streak, the LLJ, and lower tropospheric cyclogenesis. The cases which have been studied as those which occurred in the eastern United States where data coverage is more dense and the terrain is less steep. The case studied here occurred over the western and central United States. The development of a cutoff cyclone and its associated upper-level jet with a rapidly developing lower level cyclone and its LLJ over the central United States was studied in a region which has sparse data and steeply sloping terrain. For this case, output from the Eta Model was selected. The Eta Model was

chosen over the Nested Grid Model (NGM) due to the higher spatial and temporal resolution of the Eta Model to show the dynamical interactions between the upper-level low, ULJ, LLJ, and cyclogenesis.

CHAPTER III

THE ETA MODEL

This research used Eta Model sounding data from a case of cutoff cyclone development during the period 14-18 October 1994. For this case, a set of data was acquired from the National Severe Storms Laboratory in Norman, Oklahoma. These data sets were composed of 461 Eta Model hourly soundings and were available for each hour of the model production cycle up to 48 hours from the initialization time for the model. These model soundings were distributed across North America as well as over the oceans and Gulf of Mexico. For this case, the data distribution showed a high concentration of soundings available over the central United States (Fig. 1). The 0000 UTC and 1200 UTC productions for each day were available beginning at 1200 UTC on 14 October 1994 and continuing to the model production cycle at 1200 UTC on 18 October 1994.

The Eta Model (Black 1988; Mesinger et al. 1988; and Janjić 1990) replaced the Limited Area Fine Mesh Model (LFM) in June 1993 as the "NMC Early Run" guidance. This new model provides guidance over North America as quickly as possible (Black et al. 1993) and is known as the 80-km version of the Eta model. Future versions of this model will be generated at the mesoscale resolution and will run later in the production schedule (Black 1994).

The Eta Model is a quasi-hemispheric primitive equation model with a semi-

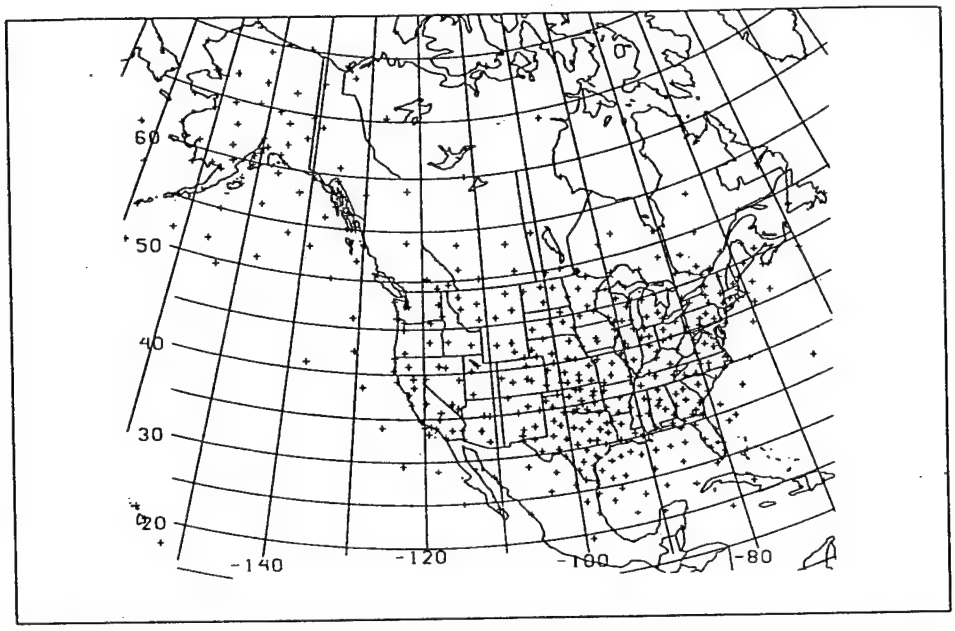

Figure 1. Location of Eta Model soundings available for this study.

staggered grid. This means that the grid values are predicted on alternate points to those of all the mass variables (e.g., temperature, specific humidity, etc.). Figure 2 shows this staggered structure where u and T represent the horizontal wind components (u and v) and the mass variables other than surface pressure, respectively. The circled u grid points indicate the points with zero values of the velocity component normal to sides of the mountain shown in the figure.

The horizontal grid resolution of the model ranges from 87.7 km at the center of the domain to 79.6 km on the northern and southern boundaries. The vertical resolution of the model is in 38 layers with the lowest layer of the model over the ocean having a thickness of 20 m for a standard atmosphere. The thickness of the layers increases with height into the middle troposphere at which point the layers begin to thin with respect to mass. Figure 3 shows the thickness of each layer. There is a secondary maximum in the thickness of the layers occurring at the 250 hPa level. This allows for a greater resolution of the vertical structure of the jet stream.

Mesinger (1984) found that it is possible to get quasi-horizontal coordinate surfaces which do not suffer the problems of the sigma coordinate system. This new coordinate system (eta) is specified as:

$$\eta = (p-p_t)/(p_s-p_t)\ \eta_s \tag{1}$$

where

$$\eta_s = (p_{rf}(Z_s)-p_t)/(p_{rf}(0)-p_t) \tag{2}$$

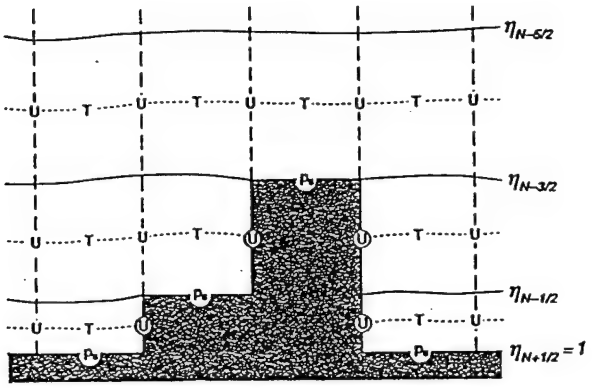

Figure 2. Conceptual model of the step topography in the Eta Model. (Adapted from Black 1994).

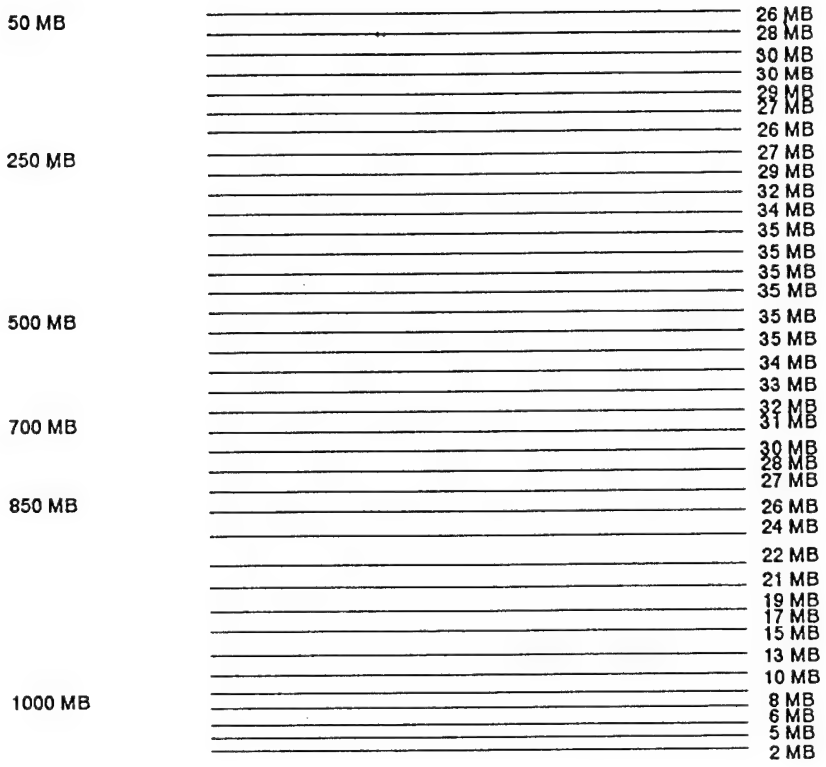

Figure 3. The 38 layers in the Eta Model with pressure on the left with respect to the standard atmosphere and the pressure depth for each level. (Adapted from Black 1988).

Here p is for pressure; the subscripts t and s represent the top and ground surface values of the model atmosphere; Z is the geometric height, and $p_{rf}(Z)$ is a suitably defined reference pressure as a function of Z; the ground surface heights, Z_s.

A. Eta Model Analysis and Initialization

The Eta Model analysis and initial conditions are aided by an optimum interpolation analysis scheme similar to those used by the current regional analysis system (DiMego 1988). The initialized fields of the Regional Analysis and Forecasting System (RAFS) are either mandatory pressure levels or the Nested Grid Model's (NGM's) sigma levels. The height values of the pressure levels are interpolated to eta surfaces using a quadratic function. A full description of the process is given by Black (1988).

The first guess for the Eta Model is provided by the Global Data Assimilation System (GDAS) (Kanamitsu 1989). The data cutoff for the model is established at one hour and 15 minutes after observation time (Black 1993). The data used in the model consist of wind profiler data, domestic aircraft (ACARS) reports, and sounding data (wind and height handled at a vertical resolution of 25 hPa), as well as all available surface and marine reports.

B. Numerical Methods and the Physical Package

There are six fundamental quantities forecast in the Eta Model. The variables are pressure differences between the surface and the top of the domain, temperature, specific humidity, the u and v components of the wind, and the turbulent kinetic energy. A complete listing of the equations is found in Black (1988). The other fields associated with the surface are accumulated precipitation, soil moisture, albedo, and surface potential temperature.

The eta coordinate system is quasi-horizontal from the viewpoint of z and p systems, and it keeps the lower boundary condition of the sigma system, yet at the same time it eliminates the undesirable aspects of the steeply sloping sigma surfaces (Janjić, 1990). The physical package incorporated in the model describes the processes of turbulent exchange, large scale and convective precipitation, surface processes and radiation.

In the Eta Model, large scale precipitation follows the standard rules. Large scale condensation occurs when the relative humidity (RH) is greater than 95%, and this is summed over each layer starting at the top of the domain. If a layer is subsaturated (RH $< 95\%$), water is evaporated into that layer, and the resulting changes in temperature and specific humidity are calculated (Black 1988). For moist processes, the Eta Model uses the Betts-Miller scheme for deep and shallow convection (Betts 1986; Betts and Miller 1986). There have been some modifications introduced to this scheme (see Janjić 1990, 1994).

The radiation scheme used in the Eta Model is the Geophysical Fluid Dynamics Laboratory (GFDL) radiation scheme. This radiation scheme is similar to the one incorporated into the NMC Medium-Range Forecast (MRF) model.

The "single bucket" method is used for the ground hydrology, and the heat flux from the surface slab into adjacent soil layers is made proportional to the net radiation at the surface. The deep ground temperature flux is estimated using a prescribed soil temperature at 2.85 m as a function of latitude and terrain elevation.

CHAPTER IV

RELIABILITY OF THE ETA MODEL DATA

When using the Eta Model initialization field in a data sparse region, a lack of "ground truth" observations in the Regional Optimum Interpolation (ROI) means that the Eta Model initialization field is weighted heavily by a preceding 6-hour forecast. This forecast may or may not be a correct representation of the atmosphere. By comparing the Eta Model initialization soundings at points where radiosonde data were available, an objective comparison of the accuracy and reliability of the data over sloping terrain was obtained. This same procedure was applied to the 12-hour forecast results.

A. Procedures

Temperature and wind data from radiosondes, the Eta model initialization, and the Eta Model 12-h forecast were compared at the mandatory levels for the period 1200 UTC 14 October to 1200 UTC 18 October 1994. Using radiosonde data as "ground truth", the Eta Model soundings at radiosonde locations were evaluated to establish the accuracy of the model soundings in their description of the atmosphere. The same procedure was performed for the 12 h forecast soundings from the Eta Model.

If the Eta Model output represented a prefect predictor of the meteorological variable in question, all the points would be located on the regression line. To test the Eta Model output, an objective analysis of the temperature, wind speed and direction was performed by doing the following test: What is the variability about the fitted regression line?

The test involved an evaluation of the Root Mean Square Error (RMSE) and the R-square value. The RMSE is an estimate of the standard deviation of the response variable about the mean. It is defined as:

$$RMSE = [(y-y_i)^2/(n-k)]^{1/2} \quad (3)$$

where y_i is the value computed by the regression equation, y is the value contained in the Eta Model sounding, n is the sample size and k is the number of parameters in the model. R-square is the coefficient of determination and is a measure of the portion of variance in the y-values explained by the regression equation (Ott 1992).

For this test, a region over the central and western United States was selected, and the radiosonde stations in the area were identified. The Eta Model soundings collocated with the radiosonde stations in this area were selected. A composite analysis of radiosonde data and Eta Model soundings was made for each 0000 UTC and 1200 UTC data set. A composite analysis of the 12-h Eta model forecast was made and compared to the radiosonde data for the valid time of the Eta Model forecast.

B. Comparison of the Temperature Data and Wind Data

For the temperature data, the RMSE varied from 0.871°C to 3.987°C with an R-square value from 0.94 to 0.99. These values were accepted as reasonable for this study. A similar test was performed using the Eta Model 12-h forecast temperature for each sounding comparing these values to the temperature data from the radiosondes for that time. The RMSE varied from 1.13°C to 3.57°C, and the R-square value ranged from 0.90 to 0.94. This range was deemed acceptable.

The test used for the temperature data was applied to the wind speed data. The RMSE was evaluated to determine the variability of the Eta Model wind speed output about an estimated value given a wind speed value from the radiosonde data. The wind speed at the mandatory levels was selected, and the RMSE varied from 3.45 m s^{-1} to 4.37 m s^{-1} with an R-square value from 0.82 to 0.87. The RMSE values appeared to be too large for this study, but a separate test for the wind at 850 hPa and 300 hPa revealed that the RMSE for the 850 hPa wind was between 1.4 and 1.9 m s^{-1} and the 300 hPa wind had a RMSE between 4.8 and 5.6 m s^{-1}. These values were considered acceptable. The R-square value ranged from 0.85 to 0.90 for the 850 hPa wind speed and the 300 hPa wind speed.

A similar test was performed using the Eta Model 12-h forecast wind speed for each sounding comparing these values to the wind speed data from the radiosonde data for that time. The RMSE varied from 1.8 to 2.5 m s^{-1} for the 850 hPa wind to 5.6 to 6.7 m s^{-1}

for the 300 hPa wind speed, and this range was determined to be acceptable for this case. The R-square value ranged from 0.80 to 0.84 for the 850 hPa wind speed and the 300 hPa wind speed.

C. Conclusions

A statistical analysis of the temperature data and wind speed data from the Eta Model was performed on the data from the Eta Model to determine the variability about the regression line. For the temperature data from the Eta Model initialization and the 12-h forecast compared to the radiosonde data, the RMSE values are reasonable. Using the same procedure for the wind speed data, the RMSE values were evaluated and were considered reasonable. For this case, the Eta Model soundings were considered a realistic representation of the atmosphere.

CHAPTER V

THE INTERACTION OF AN UPPER-LEVEL CUTOFF LOW AND A LOWER-LEVEL BAROCLINIC ZONE

The southwestern United States is a favorable region for the development of cutoff cyclones (Palmén 1949) while the region in the lee of the Rocky Mountains is a region favorable for surface cyclogenesis. When the conditions are appropriate, a surface cyclone may develop in association with an upper-level cutoff cyclone. The case of an upper-level cutoff cyclone and surface cyclogenesis was examined for the period between 0000 UTC 16 October and 1200 UTC 18 October 1994.

A. Method of Analysis

The spatial and temporal structure of a cutoff cyclone and its interaction with a lower-level potential vorticity maximum in the development of a surface cyclone was examined using initial field model soundings and forecast model soundings from the Eta Model. The high resolution soundings from the Eta Model provided an excellent view of the tropospheric and lower-stratospheric processes occurring in the interaction between the upper-level cutoff cyclone and the lower-level potential vorticity maximum. For convenience, the discussion focused on the 500 hPa and surface cyclone separately. These

features were not separate entities, but were the same system.

The Glossary of Meteorology (1959) defines a cutoff low as a cold low which has become displaced out of the basic westerly current and lies to the south of this current. In isobaric coordinates, a cutoff low appears as an isolated minimum in the height field separated from the basic westerly current, while in isentropic coordinates, a potential vorticity analysis shows the cutoff cyclone as an isolated maximum of potential vorticity separated from the stratospheric reservoir.

The case of a cutoff low and surface cyclogenesis was examined during the period 0000 UTC 16 October and 1200 UTC 18 October 1994 by constructing vertical sections of temperature, potential temperature, total wind, and potential vorticity. The time period chosen covered the period an upper-level cyclone became cut off and began to interact with a lower-level potential vorticity maximum to the time of occlusion of the surface cyclone. Since the forecast for the cyclonic event was successful, the Eta Model soundings were chosen to study the atmospheric processes.

B. Sea-Level Pressure and Upper Air Analyses

The sea-level pressure chart for 0000 UTC 16 October (Fig. 4) shows an anticyclone over eastern Canada. A stationary frontal boundary extends southward from south-central Canada into a 996 hPa low in western Colorado. A cold front extended from the cyclone in Colorado southwestward into Arizona. There was a strong southerly flow

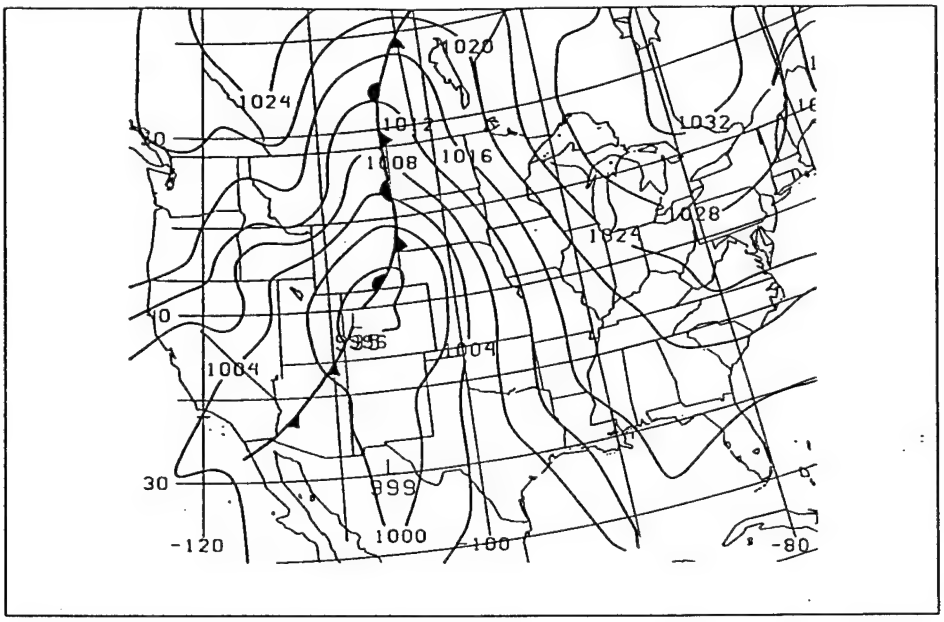

Figure 4. Sea-level isobars (in hPa) and surface fronts for 0000 UTC, 16 October 1994.

across the central United States ahead of the frontal boundary. Aloft, a cutoff cyclone center at 500 hPa was located near the Nevada-Utah border. The 500 hPa chart for this time (Fig. 5) shows a closed circulation center with a 5450 m center.

The 500 hPa low showed little movement, and there was little change in the height of the 500 hPa surface between 0000 UTC 16 October and 1200 UTC 16 October. By 0000 UTC 17 October, the 500 hPa surface in the center of the cyclone had risen by 70 m, and the cyclone had begun to move to the northeast. The 500 hPa height analysis for 0000 UTC 17 October (Fig. 6) shows a northeast-southwest elongated asymmetric cyclone. Palmén (1949) observed that a cutoff cyclone moves to the northeast after the nearly symmetric circulation of the cutoff cyclone becomes asymmetric along a north-south axis. The low over Colorado at 0000 UTC 16 October moved to the north and weakened. The 0600 UTC sea-level pressure chart (Fig. 7) for 17 October shows that cyclone with a 1007 hPa over northern South Dakota with a frontal boundary extending to the south into a 1006 hPa cyclone over southwestern Texas. The lower-level cyclone over Texas at 0600 UTC 17 October moved to the north and deepened slowly. By 0000 UTC 18 October (Fig. 8), the low had moved north into southern South Dakota with the pressure down to 1002 hPa. A cold front extended to the south from the low into western Texas, and a warm front extended to the east from the low into southern Canada. The flow over the central United States was strong and from the south, and high pressure remained over the eastern United States. The northeastward progression of the upper-level low continued, and by 0000 18 October, the cyclone was located over northeastern Wyoming. The 0000 UTC 18 October

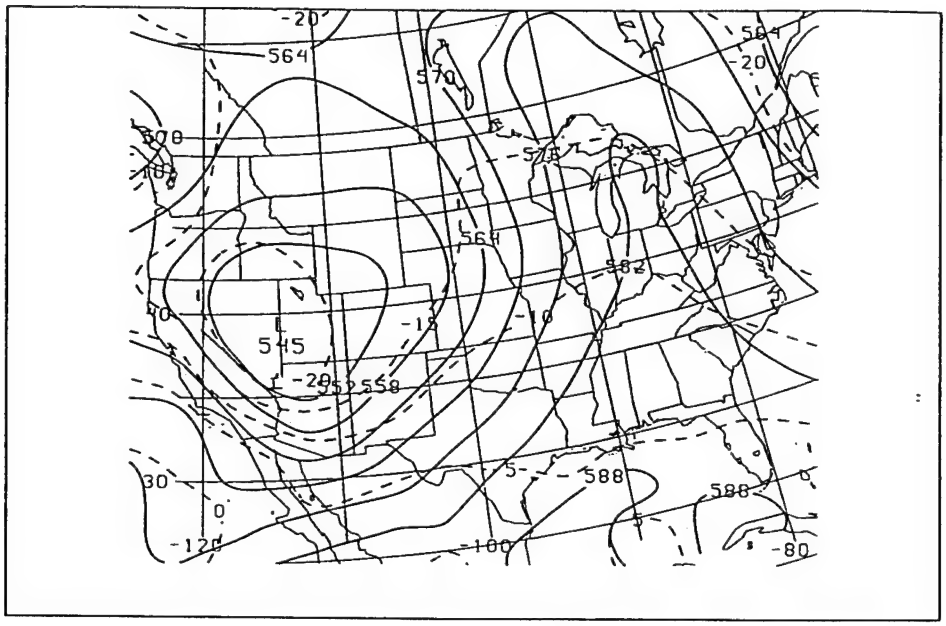

Figure 5. 500 hPa height (gp dam, solid) and temperature (dashed, °C) for 0000 UTC, 16 October 1994.

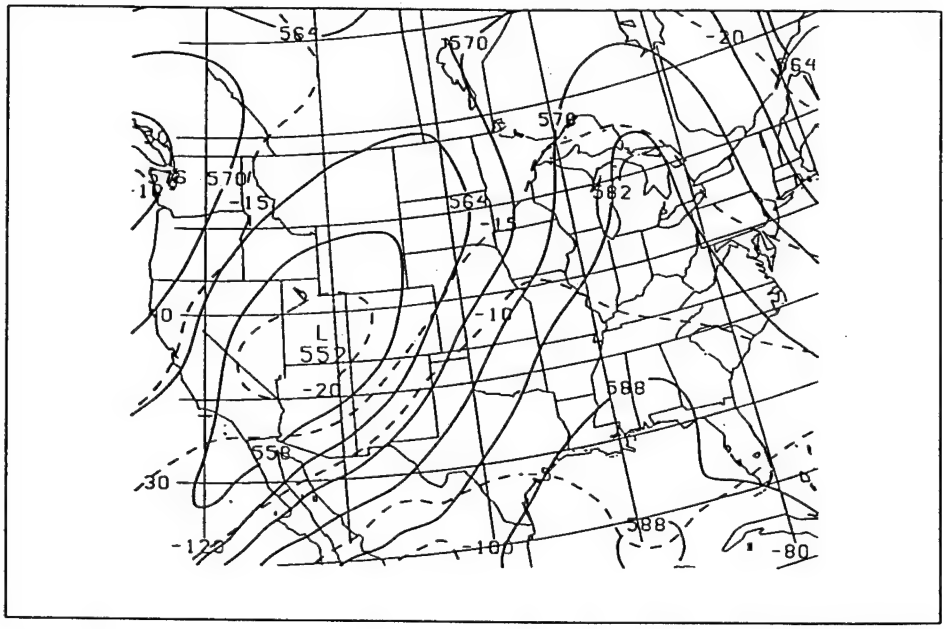

Figure 6. Same as in Figure 5 except for 0000 UTC, 17 October 1994. The 500 hPa low had become asymmetrical in the N-S axis and was moving to the east-northeast.

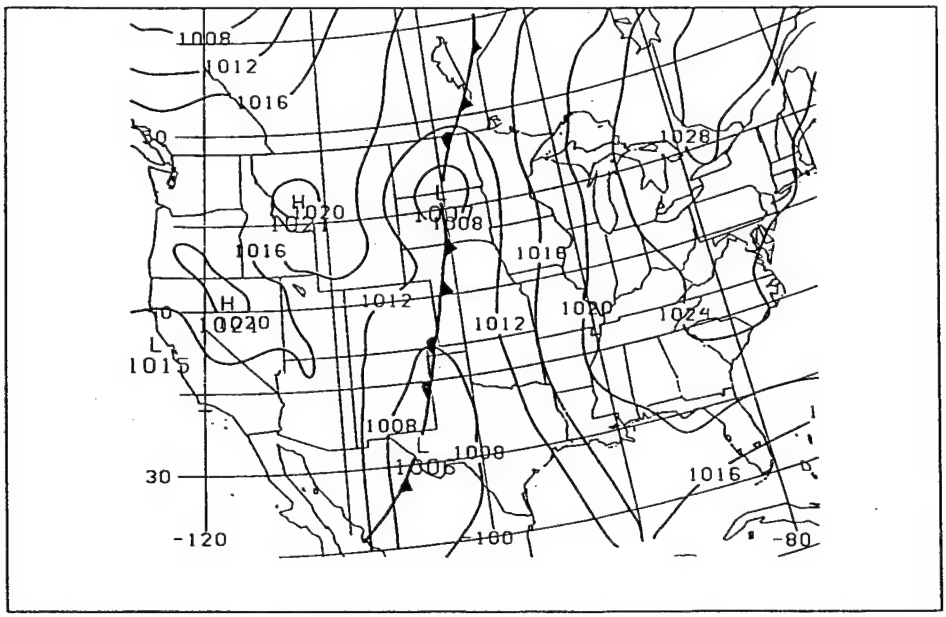

Figure 7. Same as in Figure 4 except for 0600 UTC, 17 October 1994. The wave cyclone over southwest Texas moved rapidly to the north with slow development until 2100 UTC, 17 October 1994.

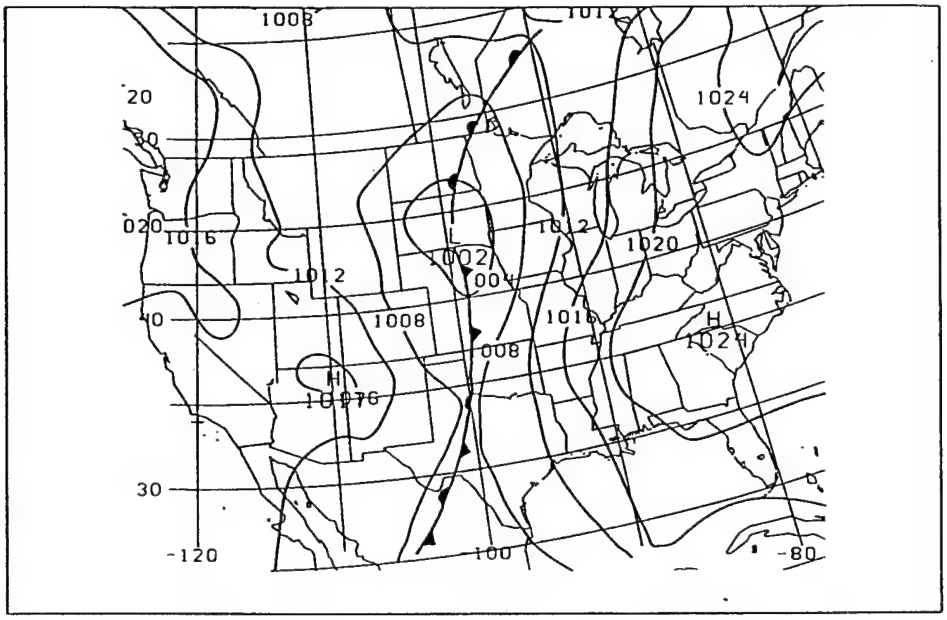

Figure 8. Same as in Figure 4 except for 0000 UTC, 18 October 1994. The pressure was falling at a rate of 1 hPa hr^{-1}.

height analysis (Fig. 9) shows the height of the 500 hPa surface at the center of the cyclone had fallen by 20 m to 5560 m. The surface cyclone deepened rapidly between 0000 UTC and 1200 UTC 18 October as it moved to the north into North Dakota. The data show that the pressure had fallen to 992 hPa and Figure 10 shows by 1200 UTC 18 October the cyclone had reached the occlusion phase of development. The closed low at 500 hPa continued to move to the northeast with the height of the 500 hPa at the cyclone center falling by 90 m. The cyclone was located over central North Dakota by 1200 UTC 18 October, and the height data of the 500 hPa surface (Fig. 11) shows that the height of the 500 hPa surface at the cyclone center had fallen to 5500 m.

C. Results and Measurements: The Isentropic Perspective

For the cyclogenesis event of 16-18 October 1994, potential vorticity was calculated and plotted on the 322 K isentropic level. The 322 K level was chosen since it represented the average surface of the tropopause during the case studied here. Potential vorticity is defined as:

$$P = -g\,(\zeta+f)(\partial\theta/\partial p) \qquad (4)$$

where P is potential vorticity, g is acceleration due to gravity (10 m s^{-2}) and $\zeta+f$ is absolute vorticity (10^{-5} s^{-1}). $\partial\theta/\partial p$ is stability, and one potential vorticity unit (PVU) corresponds

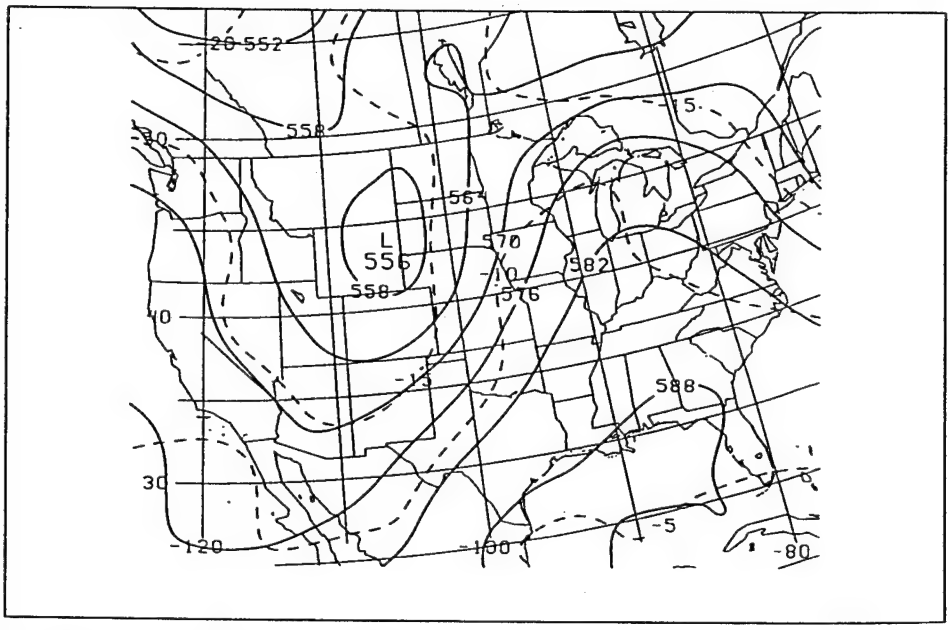

Figure 9. Same as in Figure 5 except for 0000 UTC, 18 October 1994.

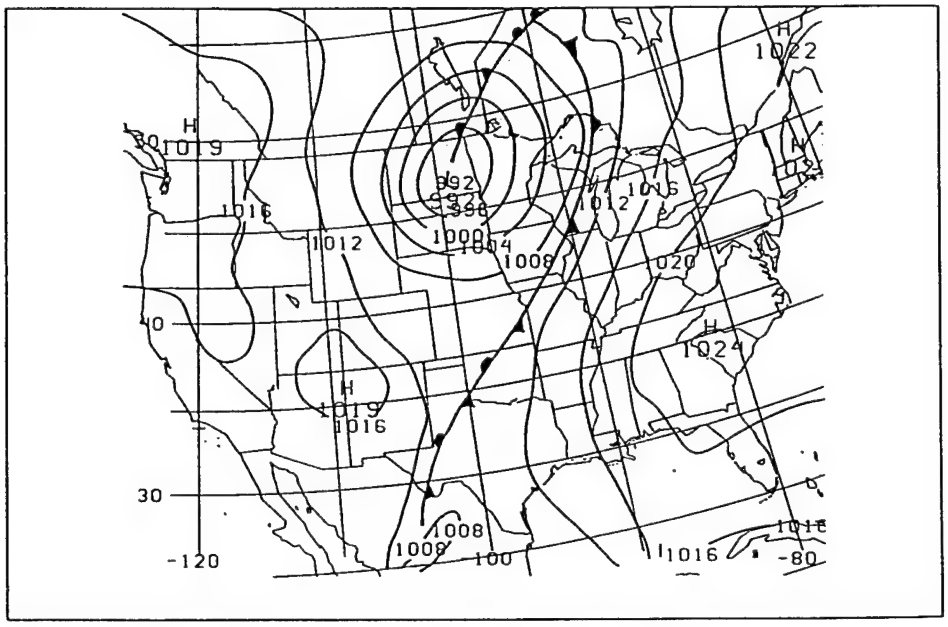

Figure 10. Same as in Figure 4 except for 1200 UTC, 18 October 1994. The pressure in the surface cyclone had reached its lowest level at this time.

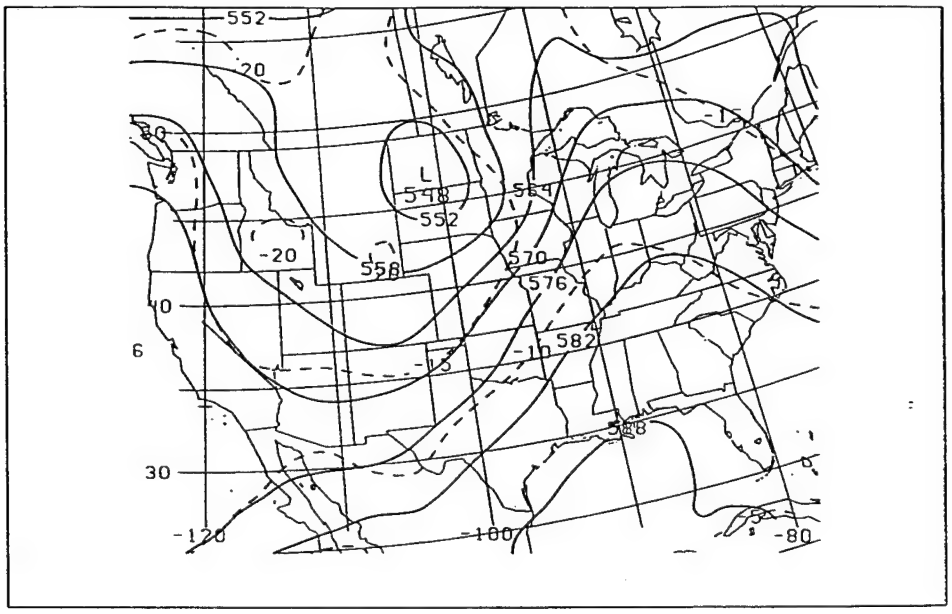

Figure 11. Same as in Figure 5 except for 1200 UTC, 18 October 1994. The height of the 500 hPa surface had fallen by 80 m in a 12-h period.

to a 10K change in θ per 100 hPa (1 PVU = 10^{-6} m^2 s^{-1} K kg^{-1}). In general, tropospheric values of potential vorticity are less than 1.5 PVU. Hoskins et al. (1985) use the 2 PVU contour to denote the tropopause, and that value was used for this cutoff cyclone case study.

An upper-level cyclone over the southwestern United States began to cut off from the westerly current by 0000 UTC 16 October. The formation of the cutoff low began when the 2 PVU contour separated from the stratospheric reservoir. Figure 12a shows the 2 PVU contour separated from the area of high potential vorticity values over southwestern Canada. An 8 PVU maximum extended from northern Nevada into southern Utah at 0000 UTC. Bell and Bosart (1993) state that the formation of a cutoff low results when a center of high potential vorticity becomes confined in the base of a diffluent long wave trough. Figures 12b-d are plots of potential vorticity on the 322 K surface at a 3-h interval beginning at 0300 UTC 16 October showing the potential vorticity maximum moving into the base of the trough. At 0300 UTC 16 October, the plot of potential vorticity (Fig. 12b) shows an 8 PVU maximum extended from southern Nevada into southern Utah, and 3 hours later (Fig. 12c), an 8 PVU maximum is located over southern Utah. By 0900 UTC 16 October, the potential vorticity analysis (Fig. 12d) shows a maximum of potential vorticity (6 PVU) was located over southern Utah in the base of the trough.

The 1200 UTC 16 October potential vorticity field (Fig. 13) shows an elongated region of potential vorticity with a maximum of potential vorticity (8 PVU) located over southern Utah. Between 1200 UTC 16 October and 0900 UTC 17 October, a maximum

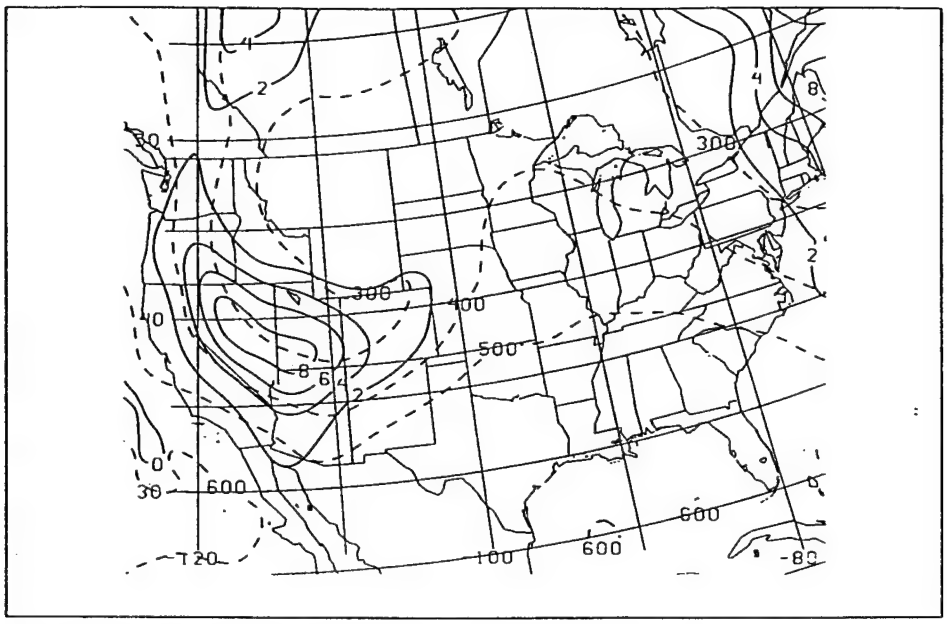

Figure 12a. Plot of potential vorticity > 1 PVU (solid, 1 PVU = 10^{-6} m^2 s^{-1} K kg^{-1}) and pressure (dashed, hPa) on the 322 K isentropic surface for 0000 UTC, 16 October 1994.

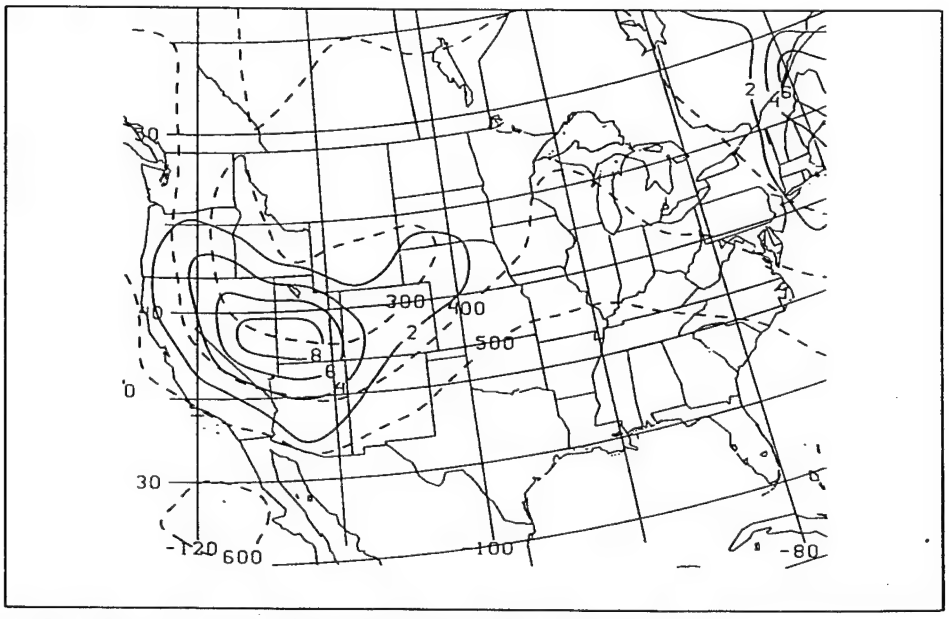

Figure 12b. Same as in Figure 12a except for 0300 UTC, 16 October 1994.

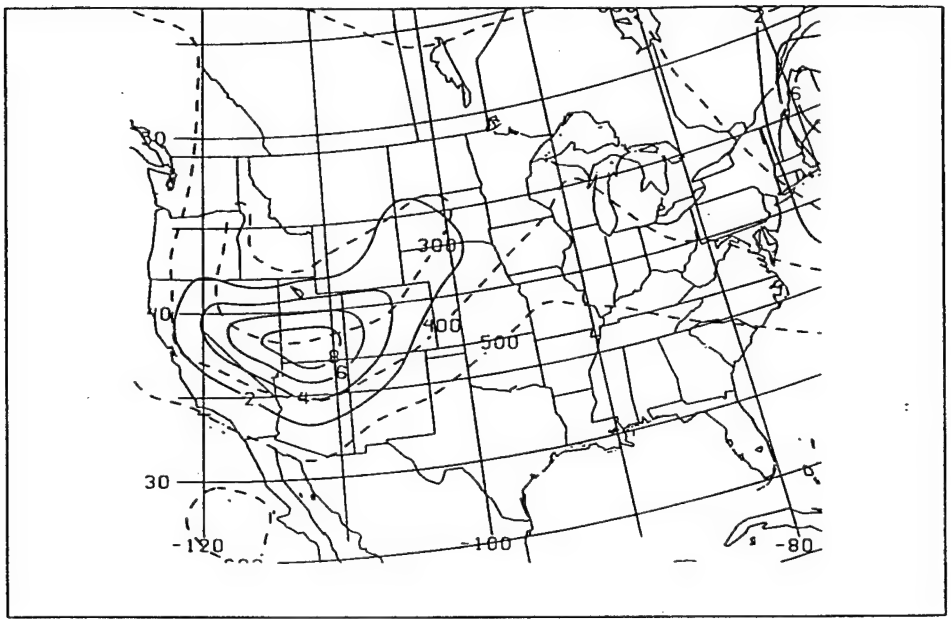

Figure 12c. Same as in Figure 12a except for 0600 UTC, 16 October 1994.

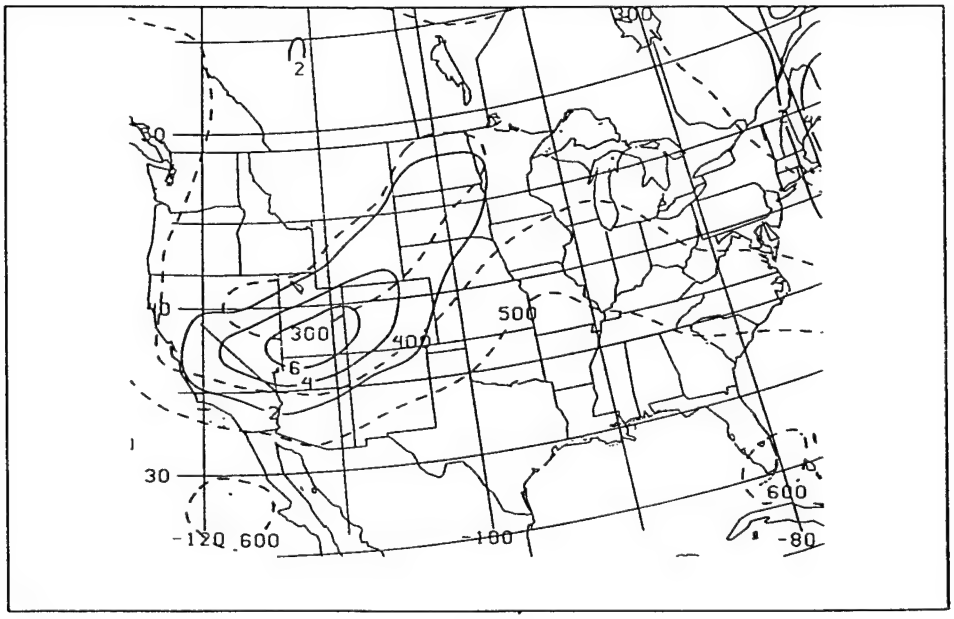

Figure 12d. Same as in Figure 12a except for 0900 UTC, 16 October 1994.

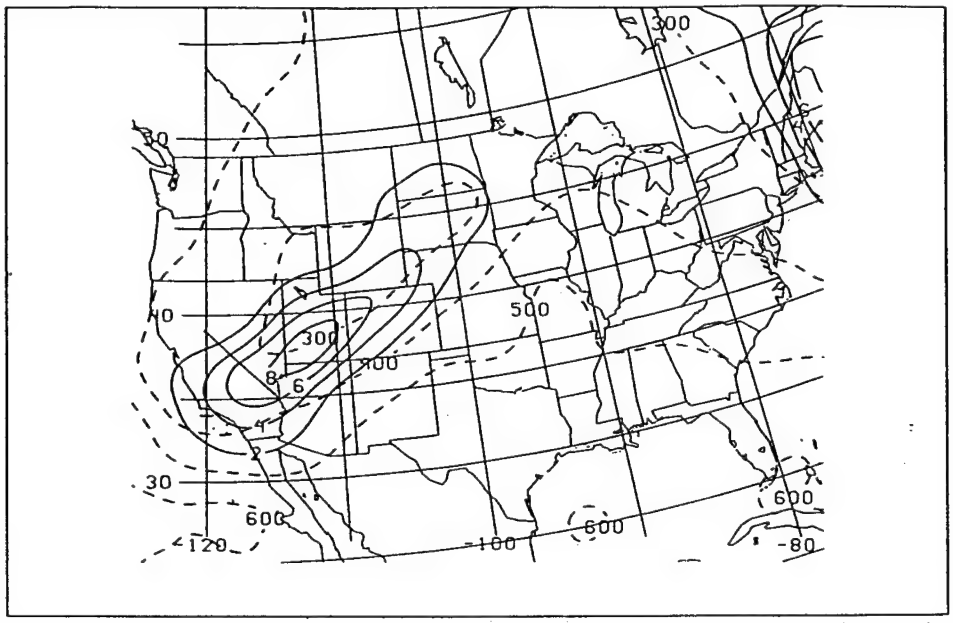

Figure 13. Plot of potential vorticity > 1 PVU (solid, 1 PVU = 10^{-6} m^2 s^{-1} K kg^{-1}) and pressure (dashed, hPa) on the 322 K isentropic surface for 1200 UTC, 16 October 1994.

of potential vorticity remained over southern Utah in the vicinity of the 500 hPa cyclone center. During this time period, there was little movement of the 500 hPa cyclone, as the cyclone remained cut off from the westerly current. Bell and Bosart (1993) state that once the center of maximum potential vorticity moves downstream of the cyclone, the cyclone should begin to weaken and move to the northeast. This case studied here followed the pattern they described.

By 1200 UTC 17 October, the potential vorticity analysis (Fig. 14) shows that the potential vorticity maximum (10 PVU) had moved to the east-northeast into eastern Utah with the 500 hPa remaining over Utah. But by 0000 UTC 18 October, the cyclone had moved to northeastern Wyoming. The movement of the upper-level cyclone was related to the northeastward movement of the potential vorticity maximum associated with the upper-level low. The potential vorticity maximum at 322 K at 0000 UTC 18 October (Fig. 15) was located to the south of the 500 hPa low. The northeastward movement of the upper-level low continued during the next 12 hours as the cyclone moved into North Dakota. The potential vorticity chart at 1200 UTC 18 October (Fig. 16) an 8 PVU maximum over northern South Dakota with the 500 hPa to the north of the potential vorticity maximum.

D. Vertical Structure of the Cutoff Cyclone

The next few figures show vertical sections through the upper-level cyclone. The

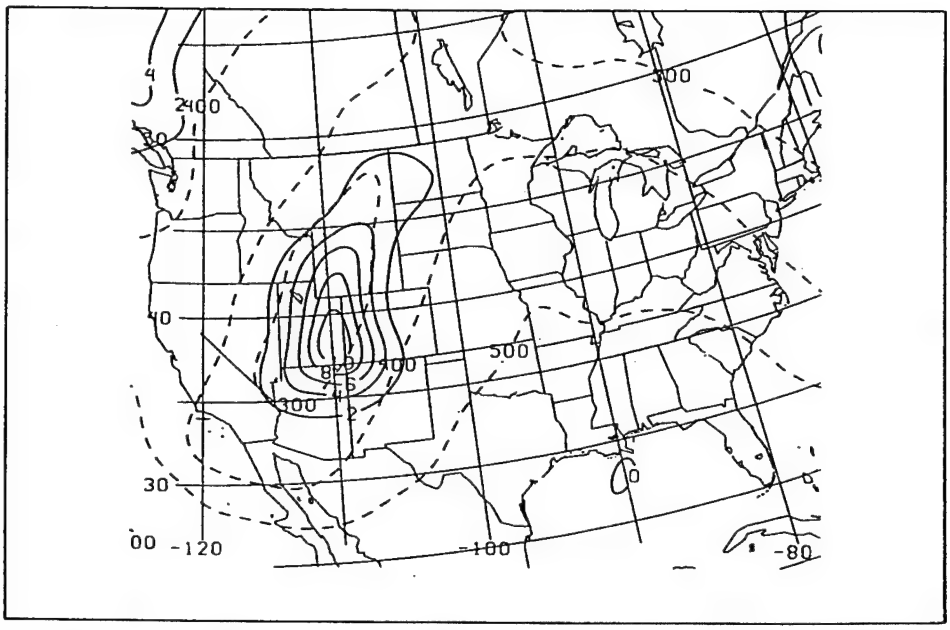

Figure 14. Same as in Figure 13 except for 1200 UTC, 17 October 1994.

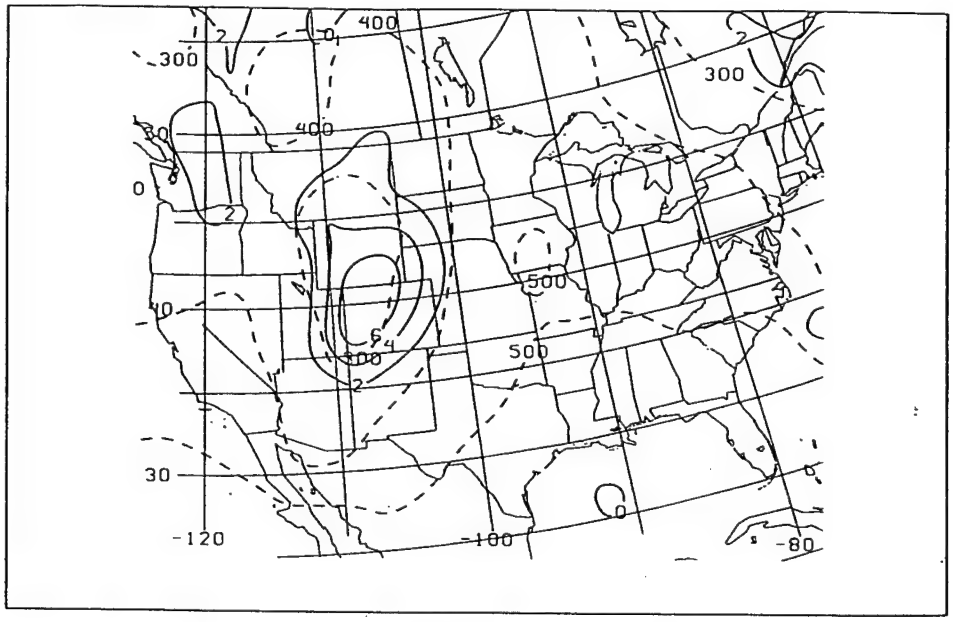

Figure 15. Same as in Figure 13 except for 0000 UTC, 18 October 1994.

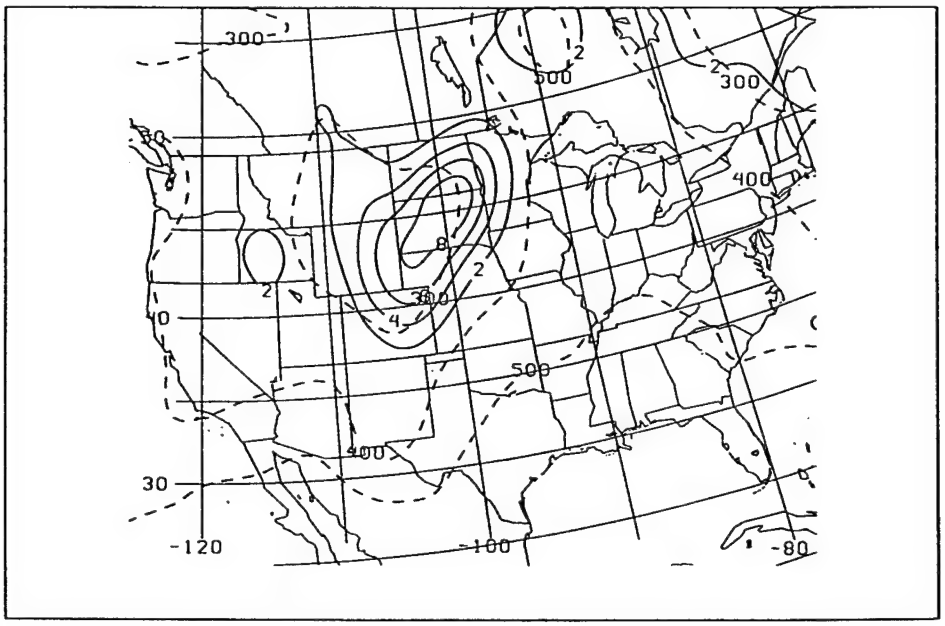

Figure 16. Plot of potential vorticity > 1 PVU (solid, 1 PVU = 10^{-6} m^2 s^{-1} K kg^{-1}) and pressure (dashed, hPa) on the 322 K isentropic surface for 1200 UTC, 18 October 1994.

sequence begins at 0000 UTC 16 October and ends at 1200 UTC 18 October 1994. These vertical sections were constructed using the model soundings from the Eta Model and show the evolution of the tropopause fold. Associated with the tropopause fold is air with potential vorticity of stratospheric values. Uccellini et al. (1985), in the case of the Presidents' Day Storm, show that air with potential vorticity values in excess of 1.5 PVU descends along the isentropes to levels as low as 700 hPa approximately 1500 km upstream of the region of cyclogenesis. In that storm, the subsidence along the Polar Front Jet contributes to the development of the fold in the tropopause 12 to 24 hours prior to intense cyclogenesis. In that study, it is shown that the descent of the high potential vorticity air aids in the intensification of the cyclone. As the stratospheric air descends into the troposphere, the air mass is stretched. The static stability of the air decreases, and the absolute vorticity increases as long as potential vorticity is conserved in the process.

The 0000 UTC 16 October vertical section of the cyclone (Fig. 17) shows that the tropopause had descended to the 500 hPa level. Potential vorticity was descending into the troposphere along the sloping isentropic surfaces. A trajectory analysis beginning at 0000 UTC 16 October (Fig. 18) shows the descent of an air parcel along the isentropic surface. A parcel with 7 PVUs starting at 295 hPa over southeastern Oregon descended to 350 hPa by 1200 UTC 16 October and was located over northern Arizona. A trajectory analysis on the 322 K isentropic level beginning at 0300 UTC (Fig. 19) shows a parcel starting in northeastern California at 350 hPa with 4 PVUs. This parcel descended to 416 hPa over western Arizona by 0900 UTC. Smoothing of the analysis and estimation of the

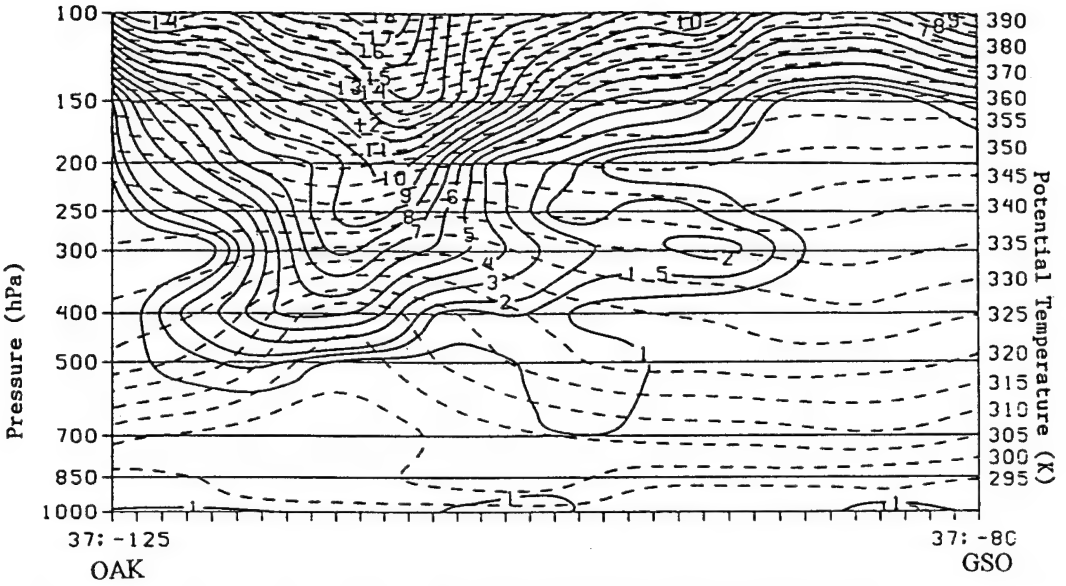

Figure 17. Vertical section showing potential vorticity (solid, PVU) and potential temperature (dashed, K) for 0000 UTC, 16 October 1994.

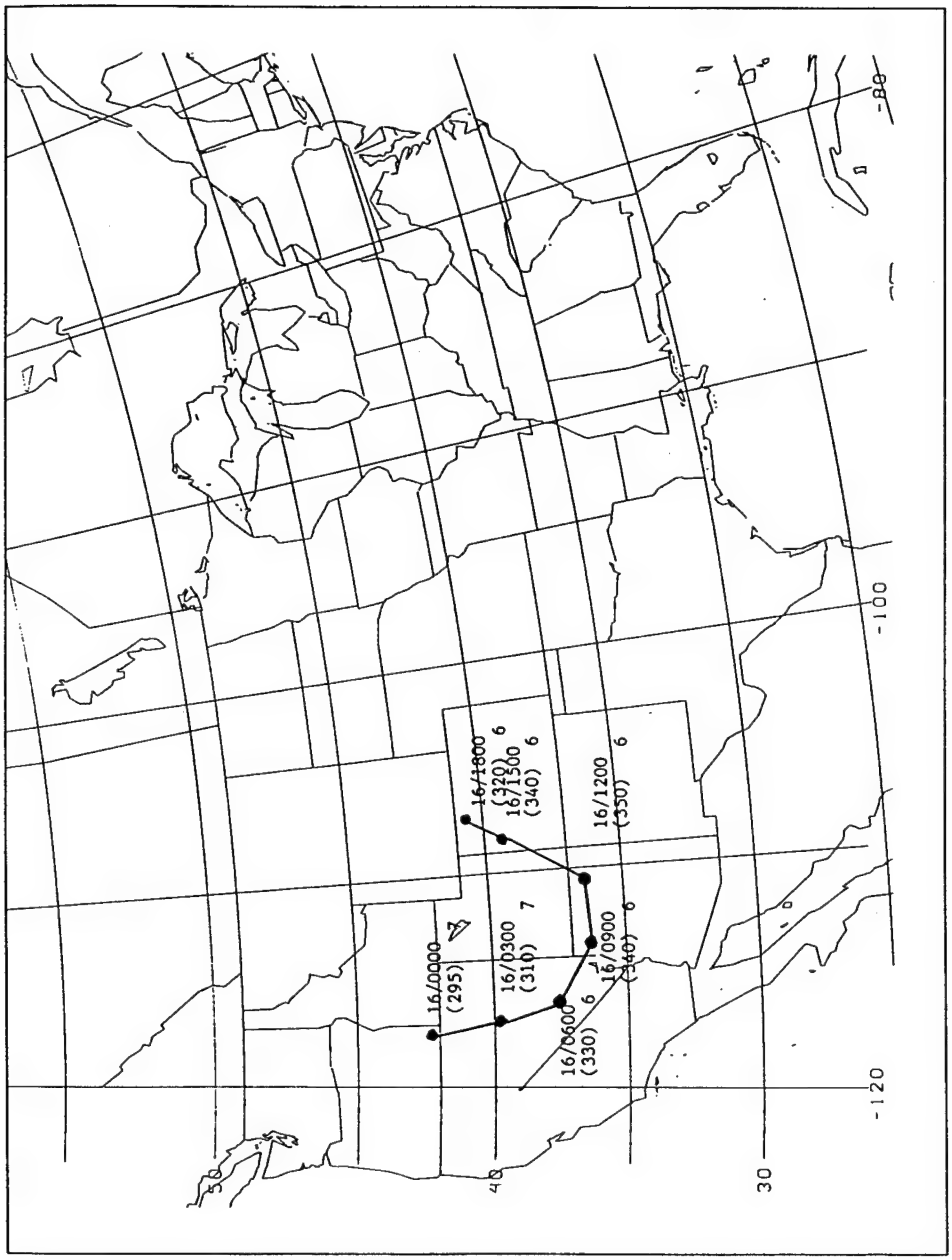

Figure 18. A trajectory on the 322 K isentropic surface at 3-h intervals starting at 0000 UTC, 16 October 1994. Pressure (in hPa) of the trajectory is shown by the three digit number in parenthesis. Potential vorticity is shown by the one digit numbers.

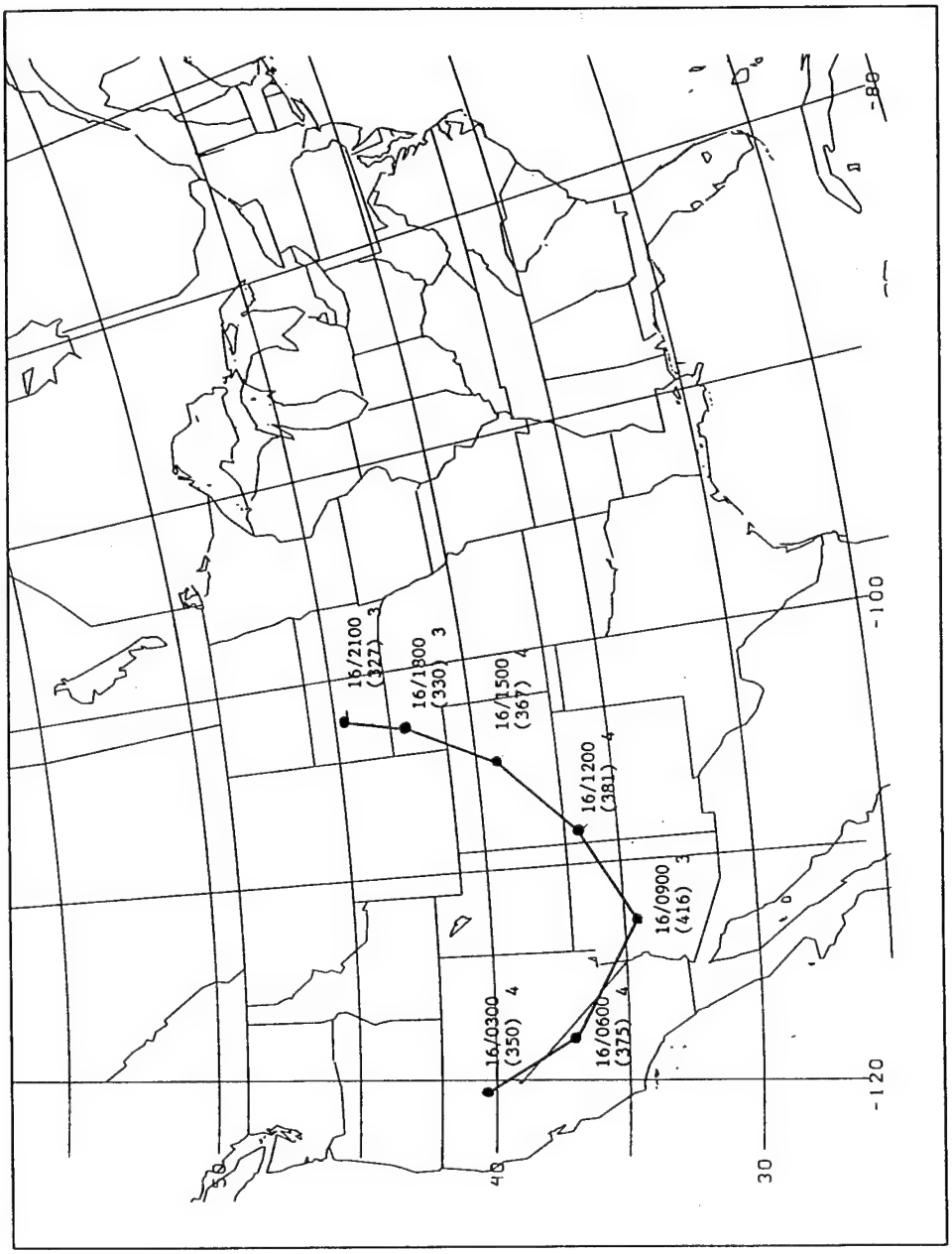

Figure 19. Same as in figure 18 except for 0300 UTC, 16 October 1994.

speed and direction of the starting and ending points of the trajectories may have resulted in the apparent failure to strictly conserve potential vorticity at this level in the atmosphere.

A vertical section through the cutoff cyclone at 1200 UTC 16 October (Fig. 20) shows that the tropopause has descended to near the 400 hPa level, and a trajectory analysis shows that the descent of potential vorticity continued into the cyclone. Figure 21 shows that a parcel starting in central Utah at 320 hPa with 2 PVUs descended to 420 hPa by 0300 UTC 17 October and moved around the southern periphery of the cyclone into southeastern Arizona.

A vertical section perpendicular to the flow at 500 hPa at 1200 UTC 16 October (Fig. 22) shows a maximum of potential vorticity (2 PVU) near the 850 hPa level. The 2 PVU maximum at 850 hPa was located over southwestern Texas. Figure 23 shows the distribution of potential vorticity at 1200 UTC 16 October on the 302K isentropic surface. The location of the 2 PVU maximum coincides with the approximate location of surface cyclogenesis 18 hours later. Hoskins et al. (1985) state that when an upper-level potential vorticity anomaly moves over a region where a low-level anomaly is situated, cyclogenesis may occur. Keyser (1986) suggests that the tropopause fold gradually extends into the lower troposphere reaching the surface downstream of the upper-level trough in the active region. Djurić (1994) states that the front assumes its usual position in the extratropical cyclone and that the cyclone develops in the active region of the trough-ridge system. Vertical sections and plots of potential vorticity on the 302 K isentropic surface indicated that the 2 PVU maximum was not maintained through the period from 1200 UTC 16

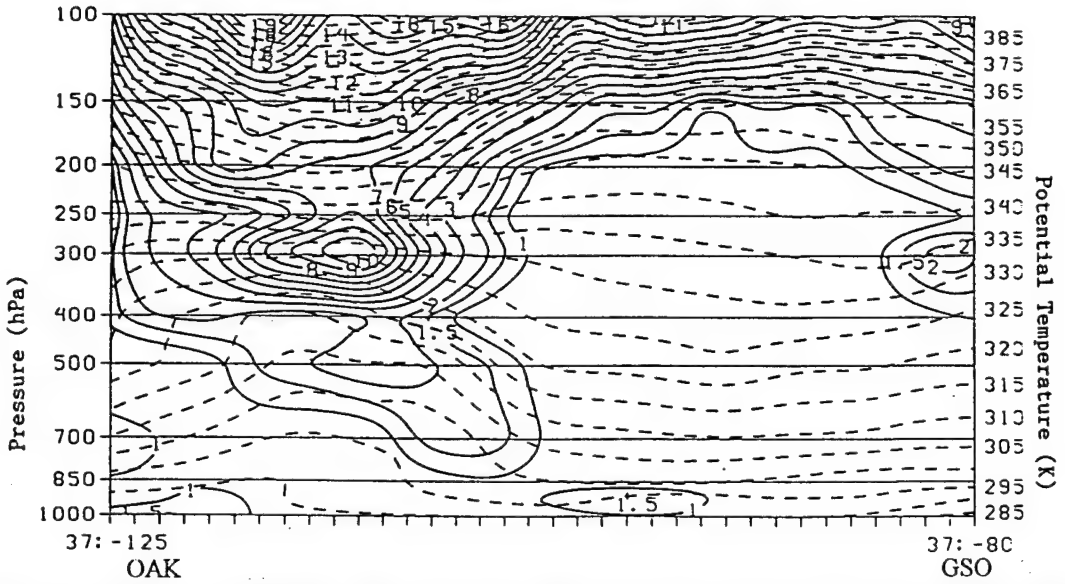

Figure 20. Vertical section showing potential vorticity (solid, PVU) and potential temperature (dashed, K) for 1200 UTC, 16 October 1994.

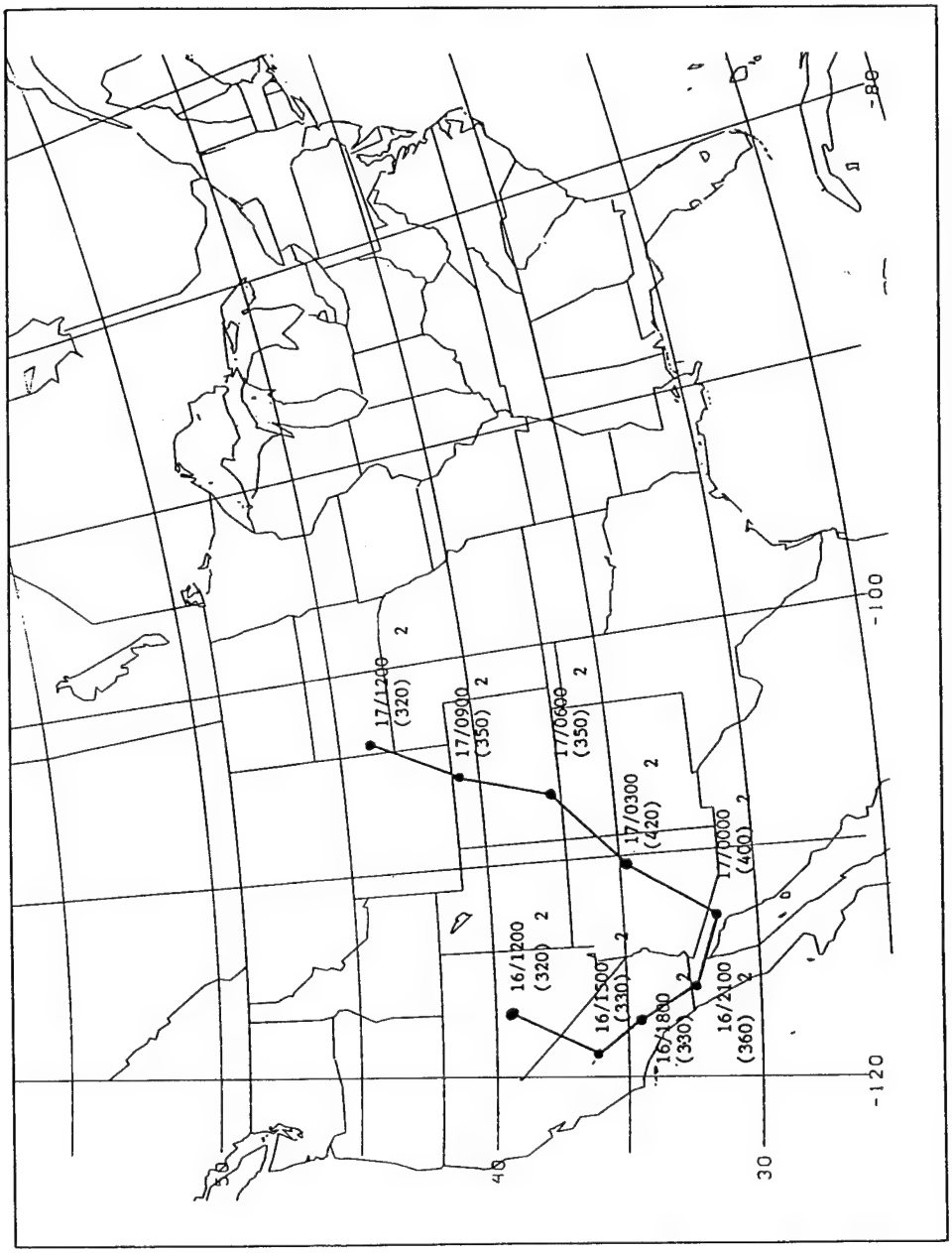

Figure 21. A trajectory on the 322 K isentropic surface at 3-h intervals starting at 1200 UTC, 16 October 1994. Pressure (in hPa) is shown by the three digit number in parenthesis. Potential vorticity is shown by the one digit numbers.

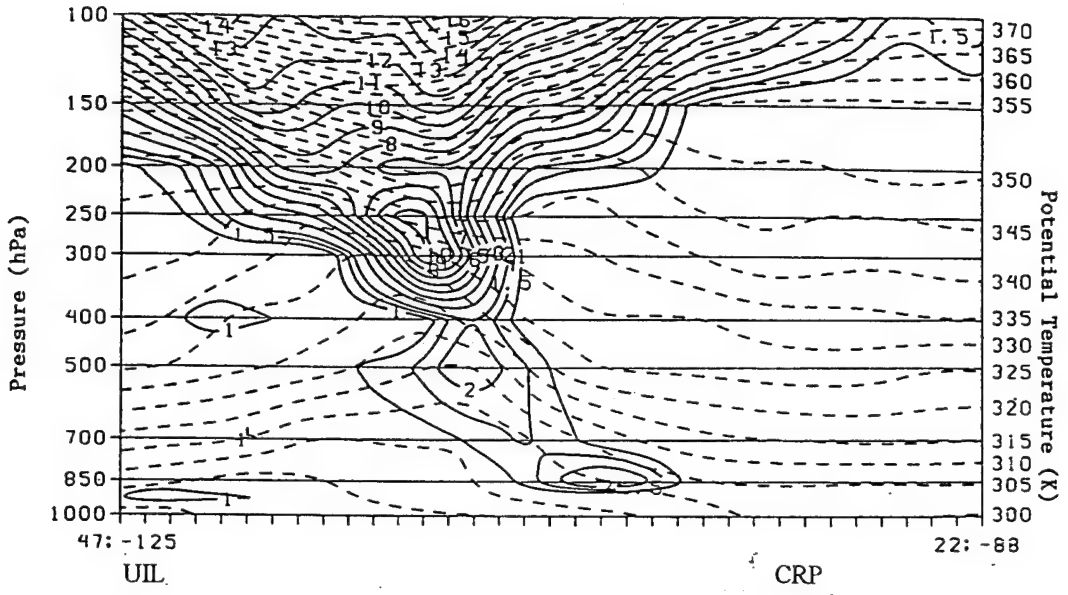

Figure 22. Vertical section showing potential vorticity (solid, PVU) and potential temperature (dashed K) for 1200 UTC, 16 October 1994.

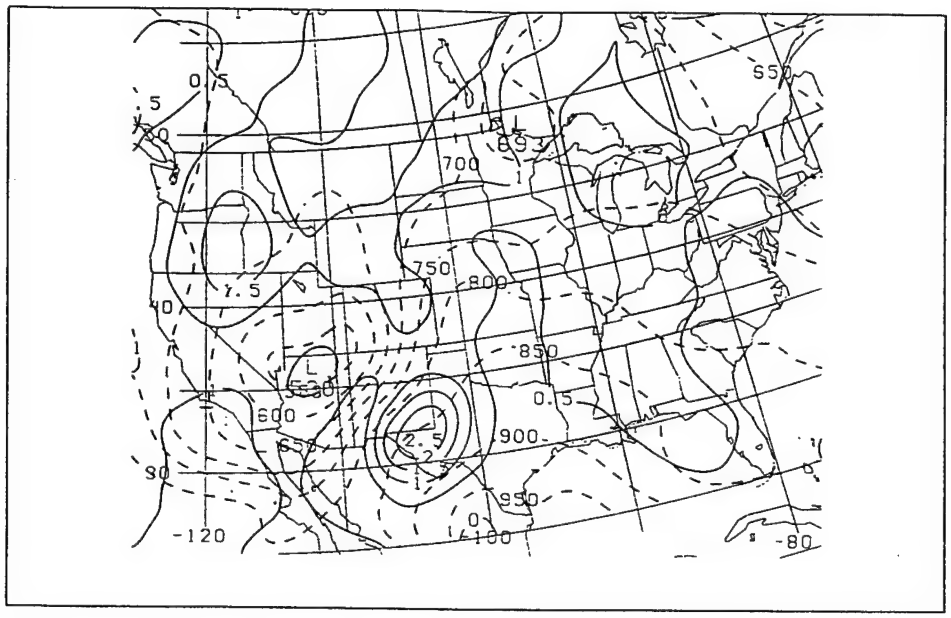

Figure 23. Isopleths of potential vorticity ≥ 1 PVU (solid, PVU) and pressure (dashed, hPa) on the 302 K isentropic surface for 1200 UTC, 16 October 1994.

October to 1200 UTC 18 October. A trajectory analysis on the 302 K surface at 1200 UTC 16 October (Fig. 24) showed that the parcel failed to conserve potential vorticity. The values of potential vorticity varied along the path of the trajectory as the parcel descended and ascended moving to the north. A possible explanation for this failure to conserve potential vorticity is that the parcel was in a region in which convection was occurring, and the release of latent heat may have resulted in a change in the potential vorticity distribution in the parcels trajectory.

Between 1800 UTC 17 October and 0900 UTC 18 October, the surface cyclone deepened and intensified rapidly with the pressure falling 15 hPa in 15 hours. The cyclone observed in this case closely approximated a cyclone defined as an explosive cyclone. An explosive cyclone is one which undergoes a pressure fall of at least 24 hPa in a period of 24 hours geostrophically adjusted to 60 degrees latitude (Sanders and Gyakum 1980).

A vertical section for 1800 UTC 17 October (Fig. 25) shows that the tropopause was near the 300 hPa level. A vertical section of the lower-level of the atmosphere at 1800 UTC 17 October (Fig. 26) shows that there was an area of high potential vorticity in the area near the surface cyclone. Hoskins and Berrisford (1988) observe that in the storm of October 1987, an upper-air potential vorticity anomaly becomes locked to a developing surface cyclone. In the subsequent development, a "potential vorticity tower" forms with the resulting cyclone developing explosively. A similar situation was observed for the case 16-18 October 1994. The 0000 UTC 18 October vertical section through the cyclone (Fig. 27) shows that the tropopause had descended to the 380 hPa level, but a vertical section

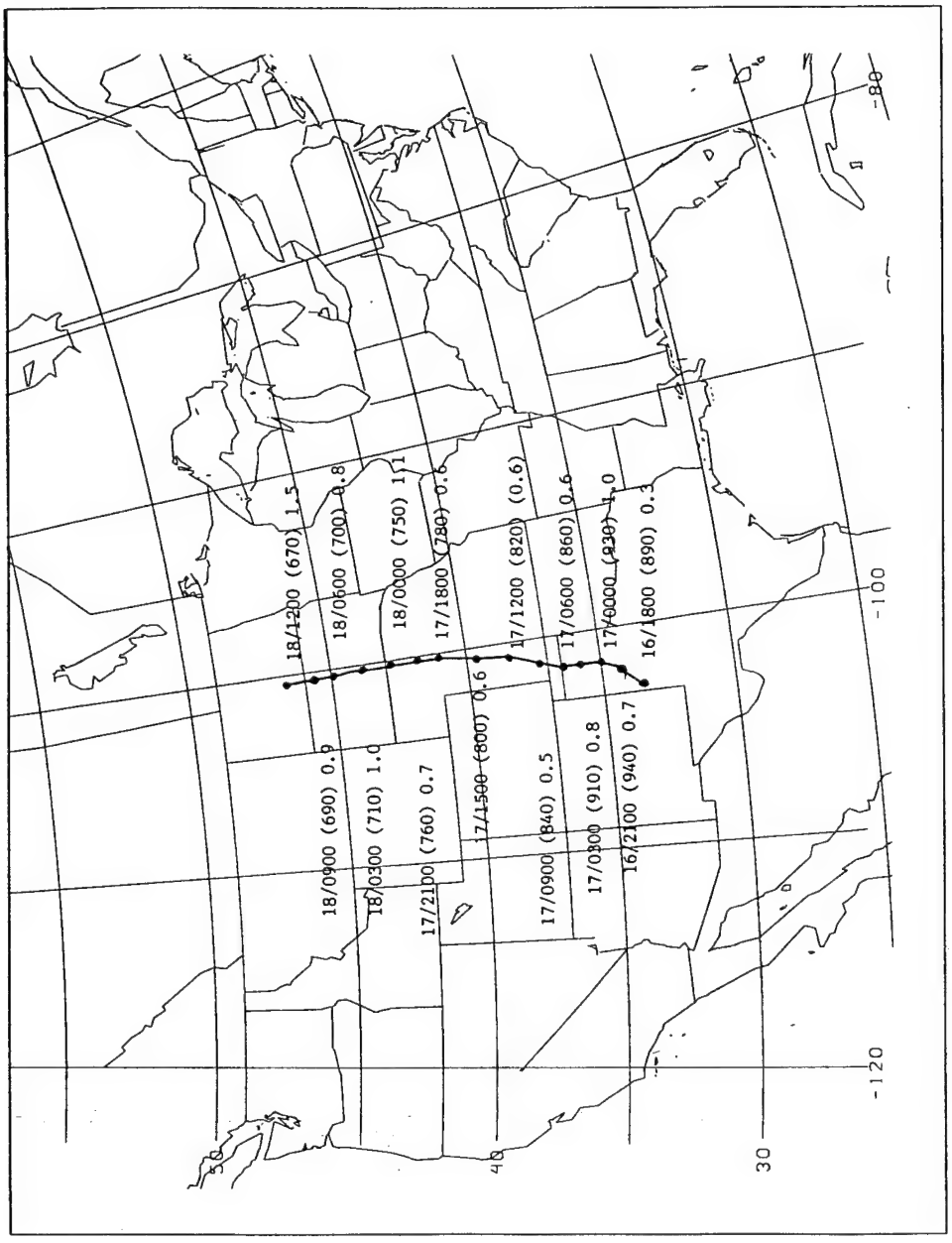

Figure 24. Trajectory on the 302 K isentropic surface at 3-h intervals starting over northwestern Texas. The pressure (in hPa) is shown by the three digit number in parenthesis. Potential vorticity is shown by the number following the pressure.

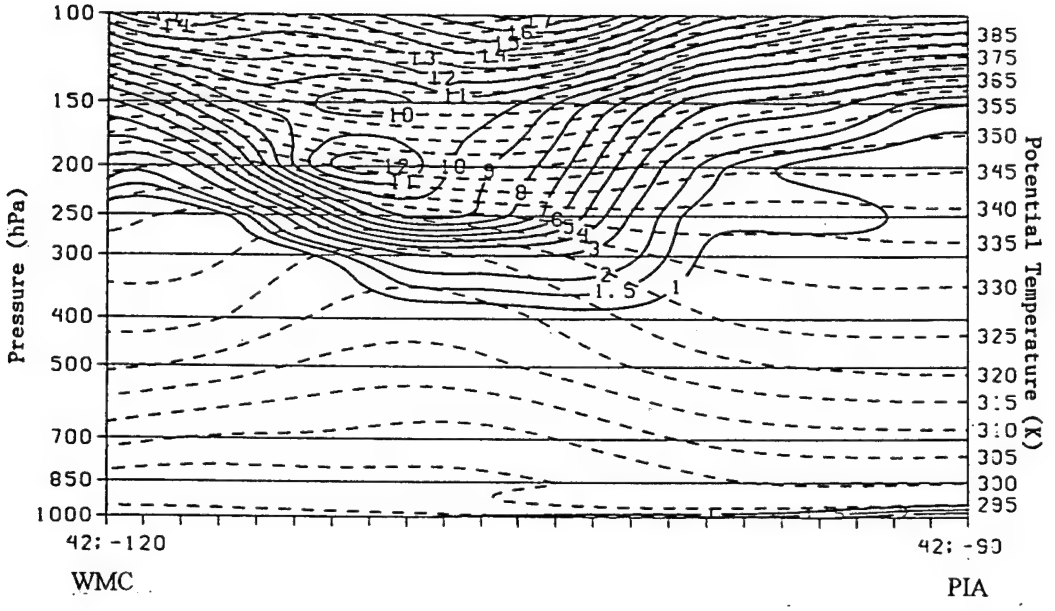

Figure 25. Vertical section showing potential vorticity (solid, PVU) and potential temperature (dashed, K) for 1800 UTC, 17 October 1994.

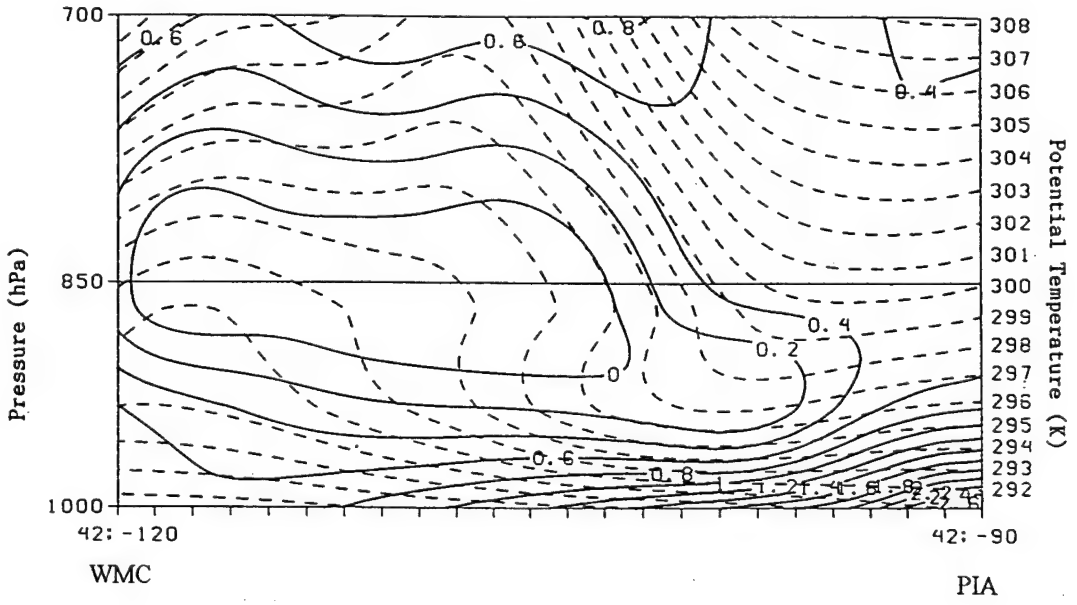

Figure 26. Same as in figure 25 except for vertical area from 1000 to 700 hPa.

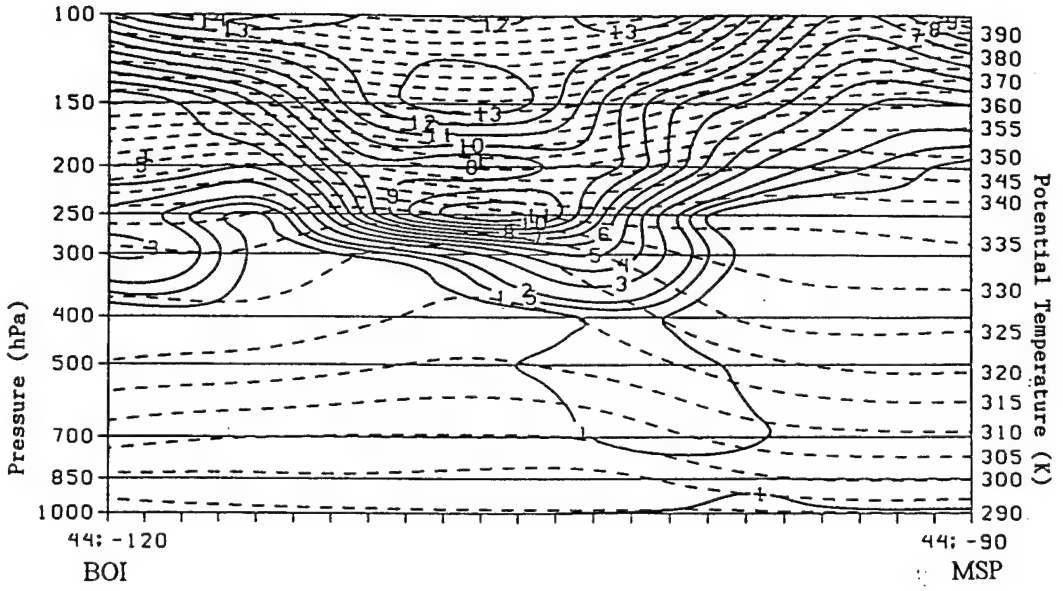

Figure 27. Vertical section showing potential vorticity (solid, PVU) and potential temperature (dashed, K) for 0000 UTC, 18 October 1994.

of the lower troposphere for 0000 UTC 18 October (Fig. 28) shows that a region of high potential vorticity greater than 1 PVU extended below the 700 hPa level. Rapid cyclogenesis was occurring during the period from 1800 UTC 17 October to 0900 UTC 18 October.

E. Conclusions

Upper-level cutoff cyclogenesis began as high potential vorticity air in the stratosphere descended into the troposphere in the vicinity of a tropopause fold. This air descended along sloping isentropic surfaces aiding in the intensification of the upper-level front and jet streak. Bell and Bosart (1993) show in a case for the GALE experiment that as the potential vorticity maximum becomes isolated in the base of the trough, the cyclone cuts off. Separation of the potential vorticity maximum from the stratospheric reservoir and isolation of the maximum in the base of the trough resulted in the cutting off of the cyclone from the flow. When the potential vorticity maximum moves downstream of the cutoff cyclone, the cyclone begins to weaken and moves to the east-northeast. Surface cyclogenesis is not observed in the case studied by Bell and Bosart (1993), but in the case for 16-18 October 1994, cyclogenesis occurred. Hoskins et al. (1985) state that when an upper-level potential vorticity maximum moves over a lower-level potential vorticity center or baroclinic zone, thermal advection by the induced lower-level circulation tends to create a warm anomaly in the lower levels ahead of the upper-level potential vorticity maximum.

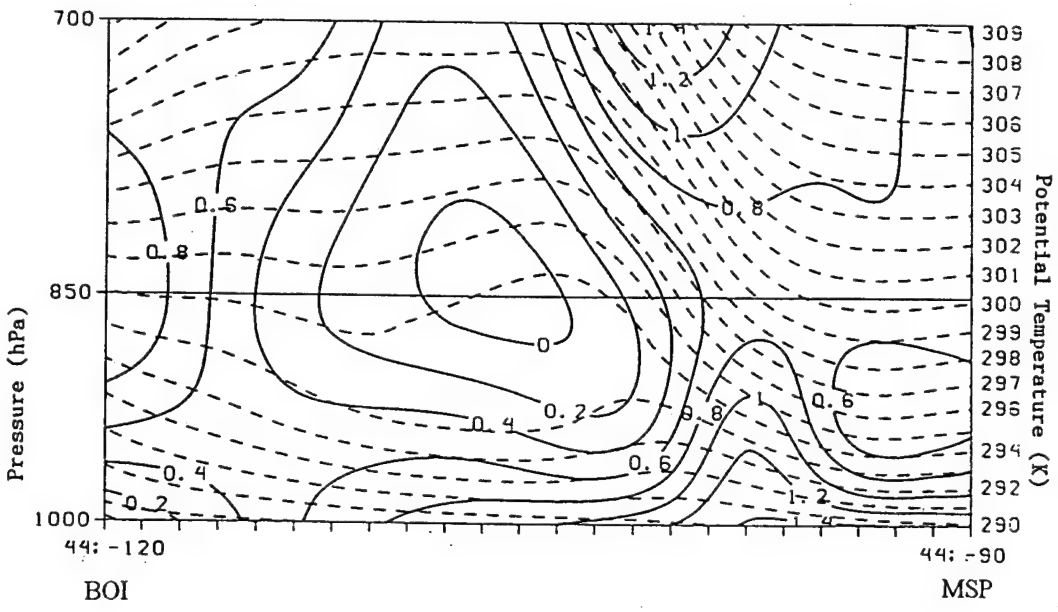

Figure 28. Same as in figure 27 except for vertical area from 1000 to 700 hPa.

The warm anomaly in the lower levels induces its own cyclonic circulation contributing in a positive manner to the upper-level circulation. As a result, an intense cyclone in the lower level develops. The lower-level potential vorticity anomaly stays ahead of the upper-level maximum with positive feedback to the upper-levels. This feedback to the upper-level cyclone helps to phase-lock the two anomalies with the result being mutual intensification. In the case for 16-18 October 1994, the upper-level potential vorticity maximum interacted with the lower-level potential vorticity anomaly over southwestern Texas, and cyclogenesis was initiated in agreement with the process described by Hoskins et al. (1985). The two anomalies appear to have interacted with a mutual intensification occurring. Rapid cyclogenesis occurred between 1800 UTC 17 and 0900 UTC 18 October with the pressure falling 15 hPa in 15 hours as a "potential vorticity tower" formed.

CHAPTER VI

THE FORMATION OF THE LOW-LEVEL JET AND INTERACTION WITH THE UPPER-LEVEL JET

The formation of LLJs has been studied quite extensively, and several mechanisms have been proposed that lead to the development of this phenomenon. The LLJ is generally found about 1 km above the ground with the maximum wind speed around 35 m s^{-1}. There are three groups of mechanisms into which these can be classified: boundary layer processes, synoptic-scale mechanisms, and orographic forcing. In this case, the synoptic-scale mechanism appears to be the primary mechanism for the evolution of a LLJ over the central United States.

A. 300 hPa and 850 hPa Surfaces

At 0000 UTC 16 October, the 300 hPa isotach plot (Fig. 29) shows a 60 m s^{-1} jet streak over western New Mexico. The cyclone at this level was located over eastern Nevada with a ridge over the eastern United States. The 0000 UTC 16 October 850 hPa isotach analysis (Fig. 30) shows a strong flow from the south with the wind speed greater than or equal to 20 m s^{-1} from Kansas northeastward to Minnesota and the temperature data showed that the 10°C isotherm (not shown) was located over northern Kansas and

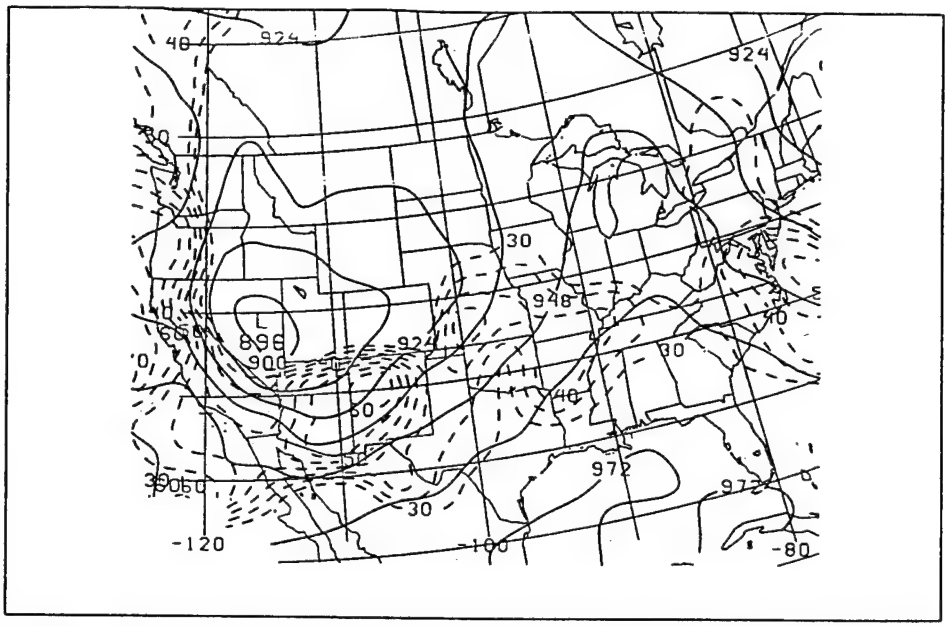

Figure 29. 300 hPa height (gp dam, solid) and isotachs (dashed, m s^{-1}) for 0000 UTC, 16 October 1994. The ridge over the eastern United States remained stationary.

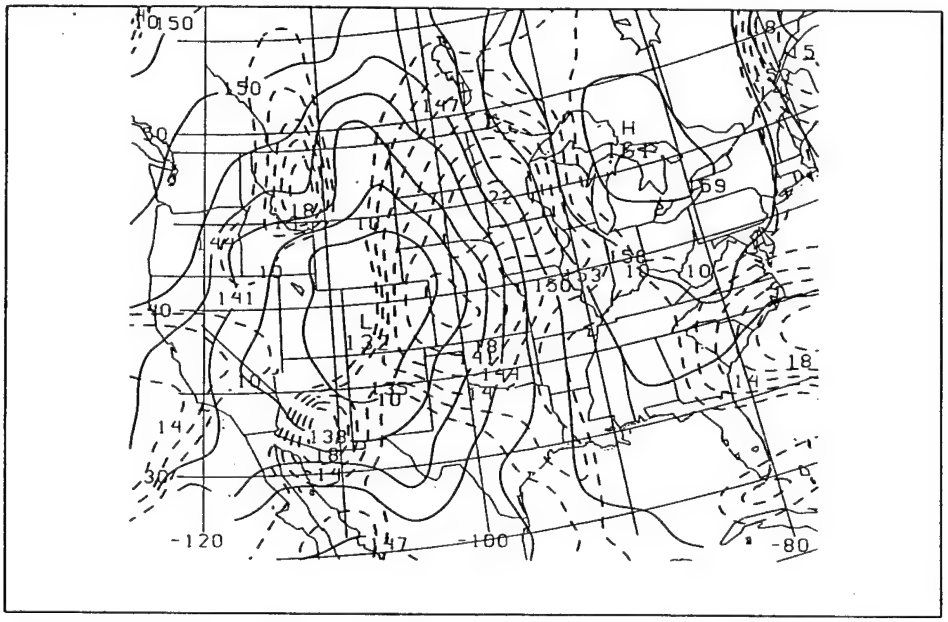

Figure 30. 850 hPa height (gp dam, solid) and isotachs (dashed, m s^{-1}) for 0000 UTC, 16 October 1994.

Missouri. By 1200 UTC 16 October, a jet streak at 300 hPa had entered the Central Plains region. The 300 hPa isotach plot for that time (Fig. 31) shows a 50 m s^{-1} jet streak had entered southwestern Nebraska with a stronger jet streak (65 m s^{-1}) over southern Arizona to the south of the 500 hPa cutoff low. The 300 hPa low was in a position close to that of the 500 hPa low. The 1200 UTC 16 October isotach analysis at 850 hPa (Fig. 32) shows that the southerly LLJ across the central United States exceeded 10 m s^{-1} with a jet streak (20 m s^{-1}) over Minnesota. The strong southerly flow was advecting warm air to the north with the 10°C isotherm (not shown) moving to the north into northern Iowa and northern Nebraska.

By 0000 UTC 17 October, the 300 hPa isotach analysis (Fig. 33) shows an elongated band of wind with speeds greater than 50 m s^{-1} extending from Arizona to Minnesota. Within this region of strong wind was a jet streak with a 65 m s^{-1} wind speed maximum over Arizona. The 300 hPa low had not moved significantly during the past 12 hours remaining over eastern Utah. Also, the ridge at this level over the eastern United States remained nearly stationary. There was a decrease in the wind speed at 850 hPa over the central United States, and by 0000 UTC 17 October, the 850 hPa isotach analysis (Fig. 34) showed that a wind speed maximum of 16 m s^{-1} extended from northeastern Kansas to southeastern South Dakota. At 1200 UTC 17 October, the 300 hPa isotach analysis (Fig. 35) shows the elongated band of winds greater than 50 m s^{-1} had not moved to the east as the ridge remained stationary over the eastern United States, but a 55 m s^{-1} jet streak extended from New Mexico into Colorado. The jet streak was no longer in the base of the

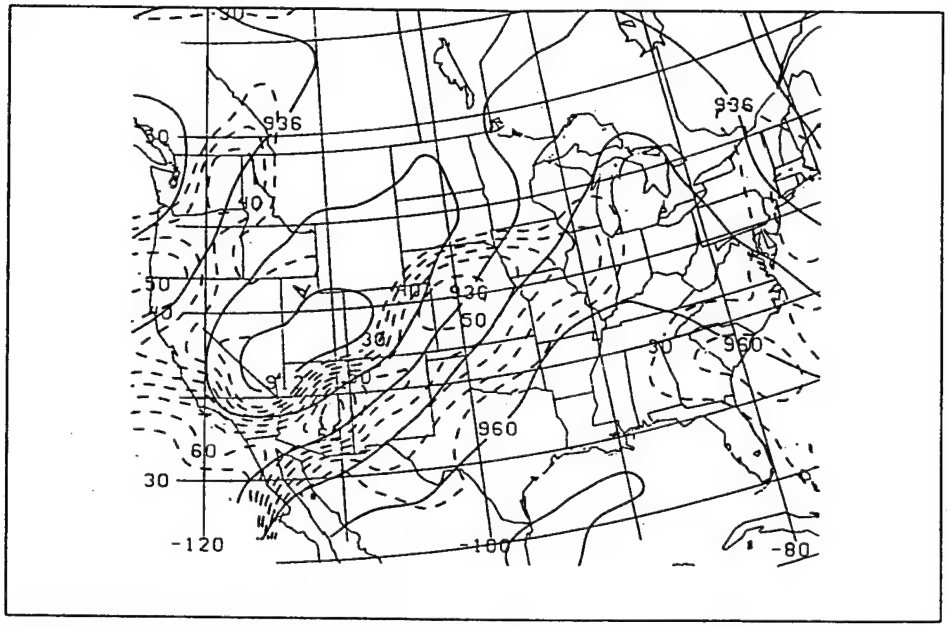

Figure 31. Same as in Figure 29 except for 1200 UTC, 16 October 1994.

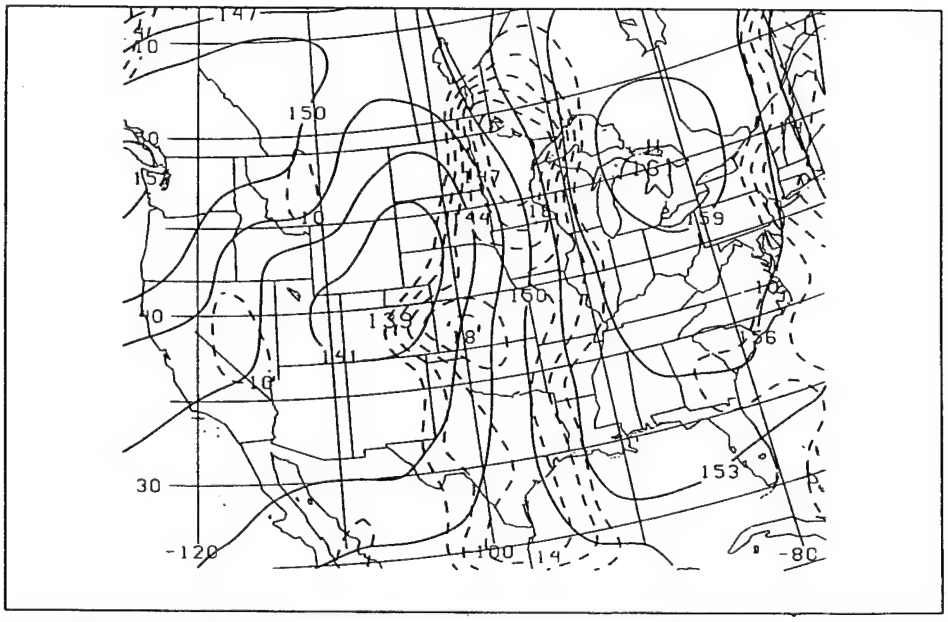

Figure 32. Same as in Figure 30 except for 1200 UTC, 16 October 1994.

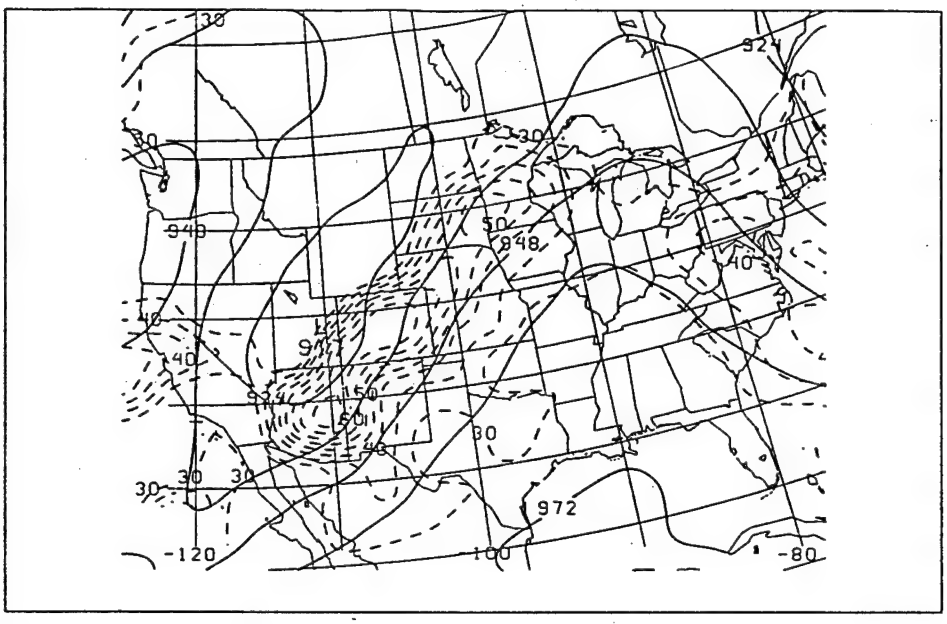

Figure 33. Same as in Figure 29 except for 0000 UTC, 17 October 1994.

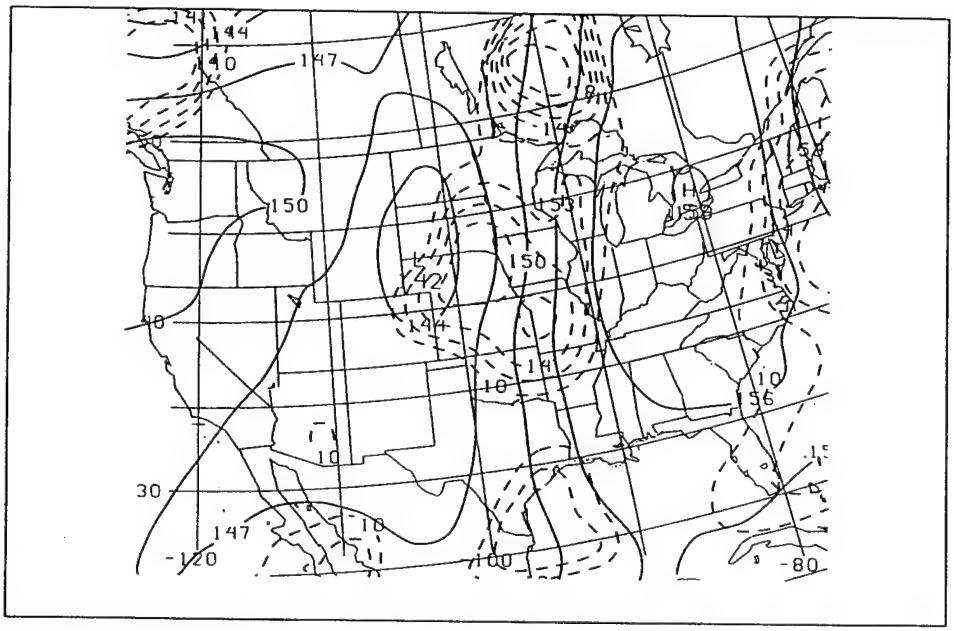

Figure 34. Same as in Figure 30 except for 0000 UTC, 17 October 1994.

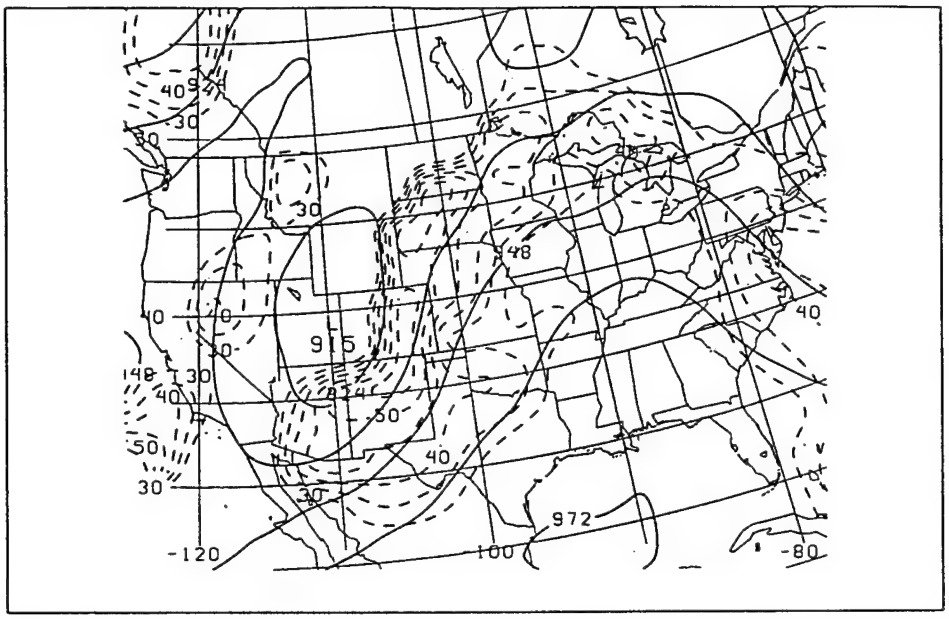

Figure 35. 300 hPa height (gp dam, solid) and isotachs (dashed, m s^{-1}) for 1200 UTC, 17 October 1994. The surface cyclone was over Southern Great Plains.

500 hPa cutoff low, and the 300 hPa low was over eastern Utah. The jet streak at 300 hPa progressed downstream of the 500 hPa cutoff low and moved to the north-northeast into the Central Plains. Between 0000 UTC and 1200 UTC, the wind speed decreased across the northern Great Plains, but there was an increase in the wind speed over the southern Great Plains in the vicinity of the developing surface cyclone. The 1200 UTC 17 October isotach analysis at 850 hPa (Fig. 36) shows a 18 m s^{-1} jet streak over northwestern Texas, and the temperature data showed that the 10°C isotherm (not shown) had moved to the north into northern Minnesota.

The 300 hPa isotach analysis at 0000 UTC 18 October (Fig. 37) shows that a 55 m s^{-1} jet streak was over southwestern Nebraska with an open wave cyclone located over southern Wyoming. At 850 hPa 0000 UTC 18 October (Fig. 38), the LLJ maximum (18 m s^{-1}) had moved to the north into northeastern Kansas and southeastern Nebraska. By 1200 UTC 18 October, the 300 hPa isotach analysis (Fig. 39) shows that the band of wind in excess of 50 m s^{-1} extended from northwestern Texas into southern Minnesota with a jet streak of 55 m s^{-1} over western Kansas. The 300 hPa low had moved into southern North Dakota; this position was close to the position of the occluded surface cyclone. The jet streak at 850 hPa had moved to the north, and the isotach analysis at 1200 UTC 18 October (Fig. 40) showed a 20 m s^{-1} jet streak had moved into southern Minnesota. The LLJ had advected warm air far to the north as the 10°C isotherm (not shown) extended into southern Ontario.

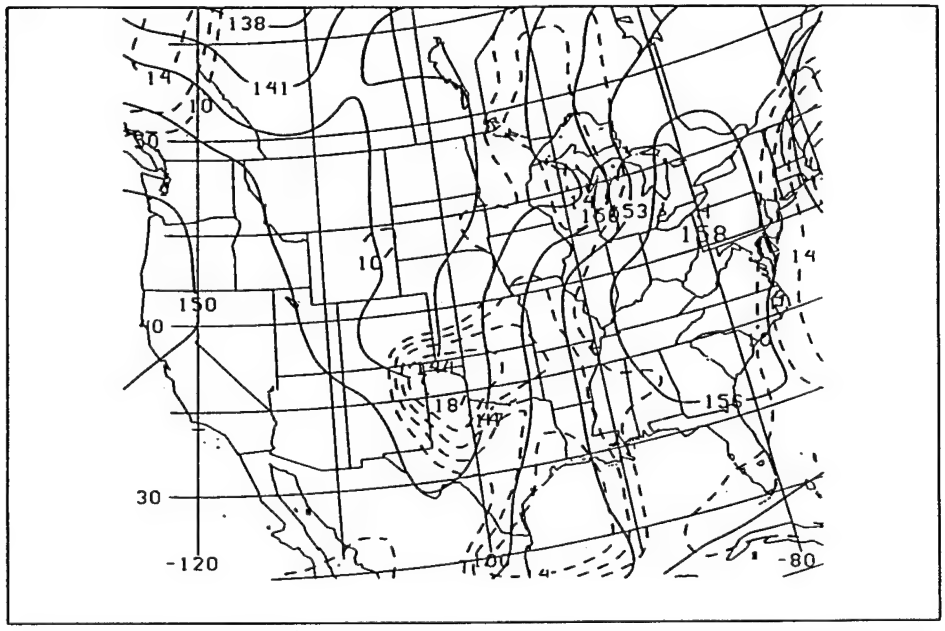

Figure 36. 850 hPa height (gp dam, solid) and isotachs (dashed, m s^{-1}) for 1200 UTC, 17 October 1994. The LLJ was located in the vicinity of the surface cyclone which was over the Southern Great Plains.

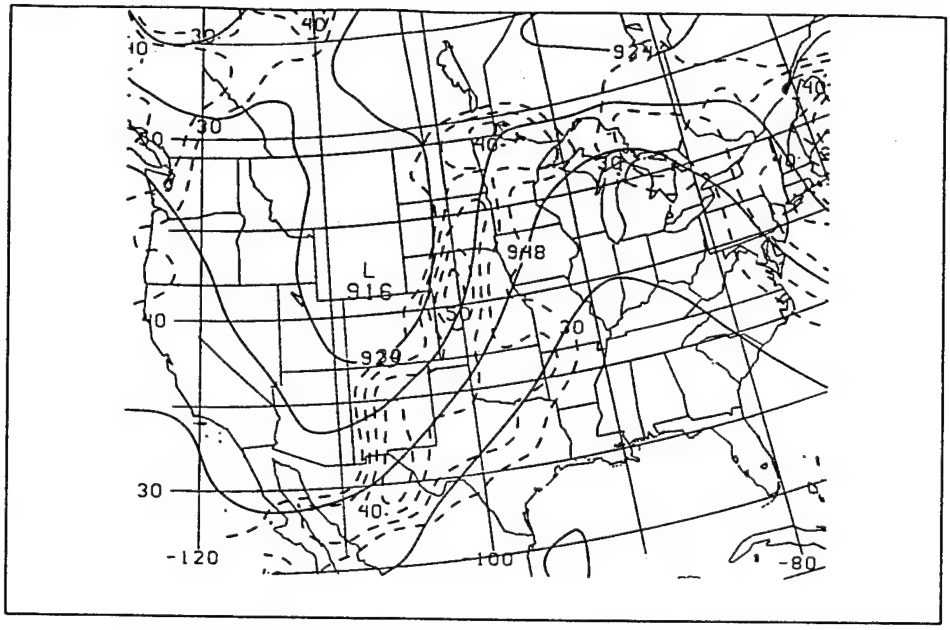

Figure 37. Same as in Figure 35 except for 0000 UTC, 18 October 1994.

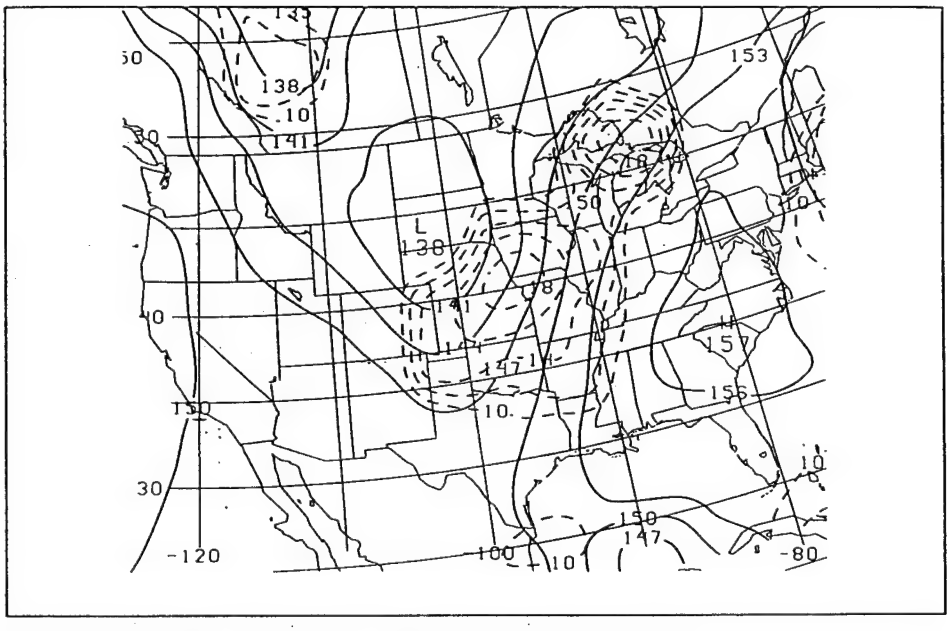

Figure 38. Same as in Figure 36 except for 0000 UTC, 18 October 1994.

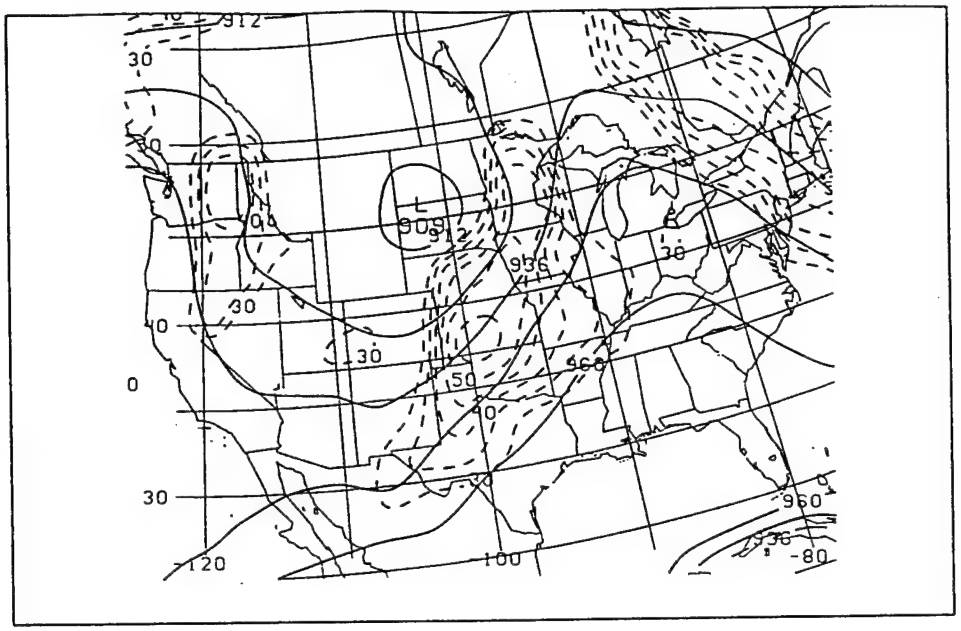

Figure 39. Same as in Figure 35 except for 1200 UTC, 18 October 1994.

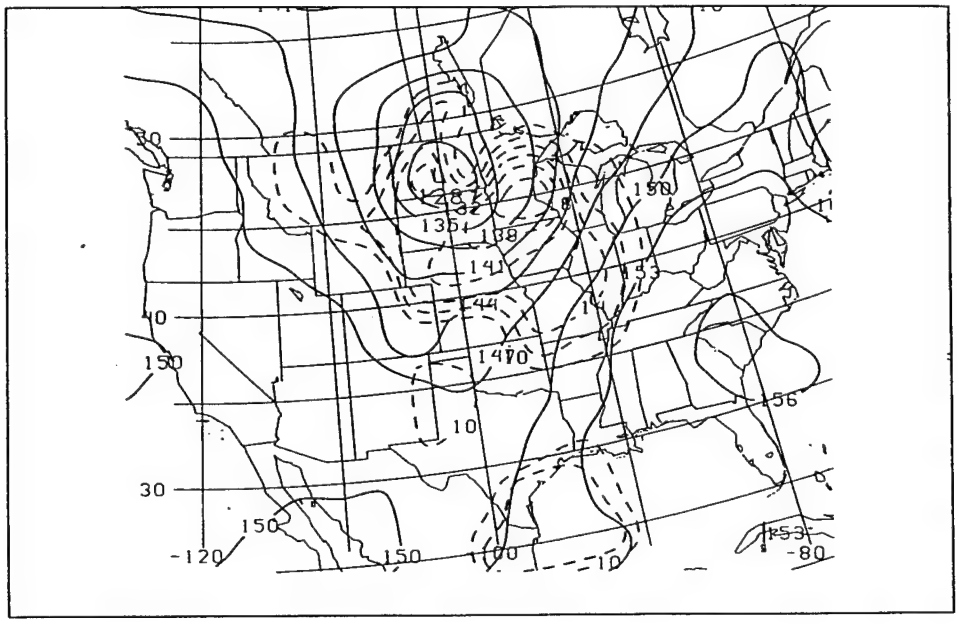

Figure 40. Same as in Figure 36 except for 1200 UTC, 18 October 1994.

B. Synoptic-Scale Forcing

The upper-level features associated with the case for 16-18 October 1994 are similar to those described by Uccellini (1980). He calls the LLJ which develops a Type 1 LLJ. The Type 1 LLJ is described as being forced by large-scale motion as opposed to the Type 2 LLJ which is a jet driven by boundary layer processes..

Many researchers have studied the development of the LLJ from the boundary layer view point. But strong synoptic-scale forcing is noted as a mechanism for the development of the LLJ by Beckman (1973), Uccellini and Johnson (1979), Djurić and Damiani (1980), Djurić and Ladwig (1983), and Uccellini et al. (1987). These authors show the LLJ development from different synoptic-scale features.

1. Upper-level jet streaks and the isallobaric wind

Uccellini and Johnson (1979) and Djurić and Damiani (1980) studied the development of the LLJ as an isallobaric flow. They show that there is an ageostrophic wind with a large isallobaric wind component in the lower atmosphere as a result of the indirect circulations associated with the exit region of a propagating upper-tropospheric jet. Acceleration of the flow results in a convergence of the flow into isallobaric lows and divergence from isallobaric highs. The LLJ tends to accelerate toward height falls and decelerate in regions of height rises.

To study this phenomenon, the geostrophic wind at 850 hPa was calculated using the definition:

$$\mathbf{V}_g = (g/f)\mathbf{k} \times \nabla z \tag{5}$$

Interpolating the observed wind, **V**, onto the same grid as that used for the geostrophic wind, the calculation for the ageostrophic wind was made:

$$\mathbf{V}_a = \mathbf{V} - \mathbf{V}_g \tag{6}$$

The isallobaric flow was calculated using the following definition:

$$\mathbf{V}_a = -(1/f^2)\nabla_p(\partial\Phi/\partial t) \tag{7}$$

where $\mathbf{V}_a$ is the ageostrophic wind, f is the Coriolis parameter, and $\partial\Phi/\partial t$ is the tendency in the geopotential height with respect to time. This equation incorporates the acceleration which results from the change of the geostrophic wind over a time period $\Delta t = 12$ h on a constant pressure surface.

At 1200 UTC 17 October, a weak isallobaric flow with a southerly component was evident over the Texas and Wisconsin. A plot of the 850 hPa 12 hour isallohypses at 1200 UTC 17 October (Fig. 41) shows that the 850 hPa surface fell by 10 m over Oklahoma and

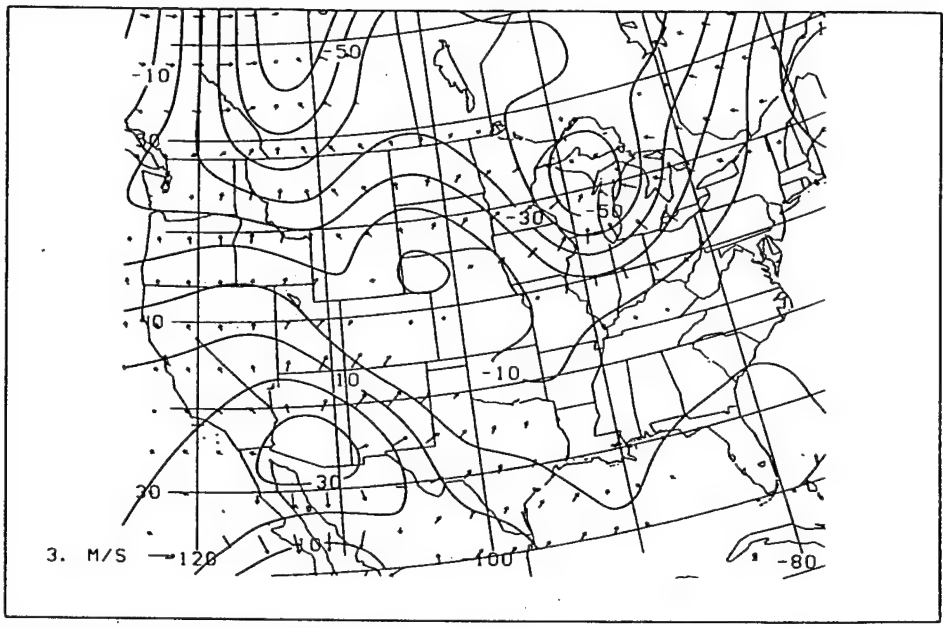

Figure 41. Plot of 850 hPa 12 hour height change (solid, gpm) and isallobaric wind (m s^{-1}) for 1200 UTC, 17 October 1994.

by 50 m Wisconsin. During the next 12 hours, the isallobaric component of the flow increased to nearly 2 m s^{-1} over Kansas. Figure 42 shows that between 1200 UTC 17 October and 0000 UTC 18 October there was a height fall of 40 m at 850 hPa over central Nebraska. Also, there was an increase in the wind speed with the wind at Omaha, Nebraska increasing from 10 m s^{-1} to 18 m s^{-1} in 12 hours. The area of the height fall corresponds to the area in which the developing cyclone was moving through as the low-level cyclone moved north from southwestern Kansas. The 850 hPa height fall center moved to the north as the low-level cyclone began to undergo rapid deepening. By 1200 UTC, the height fall center at 850 hPa had move into eastern North Dakota and western Minnesota. The isallohypses plotted for the period from 0000 UTC 18 October to 1200 UTC 18 October (Fig. 43) show that the height of the 850 hPa surface had fallen by 70 m. Figure 43 shows that the isallobaric component of the ageostrophic wind was 3 m s^{-1}. The observed wind at 850 hPa at St Cloud, Minnesota had increased from 9 m s^{-1} to 23 m s^{-1} in 12 hours.

The coupling of the upper-level jet and lower-level jet was examined by following a procedure described by Uccellini et al. (1984) for the Presidents' Day Storm. In a vertical cross-section through the subtropical jet (STJ) they show that in the cold air the vertical motion is upward, and in the warm air, the vertical motion is downward. This indicates that the circulation is a thermodynamically indirect one near the exit region of the STJ. A similar pattern was observed in the case for 16-18 October 1994. A vertical cross-section for the time 0000 UTC 18 October (Fig. 44) was constructed through the exit region of a

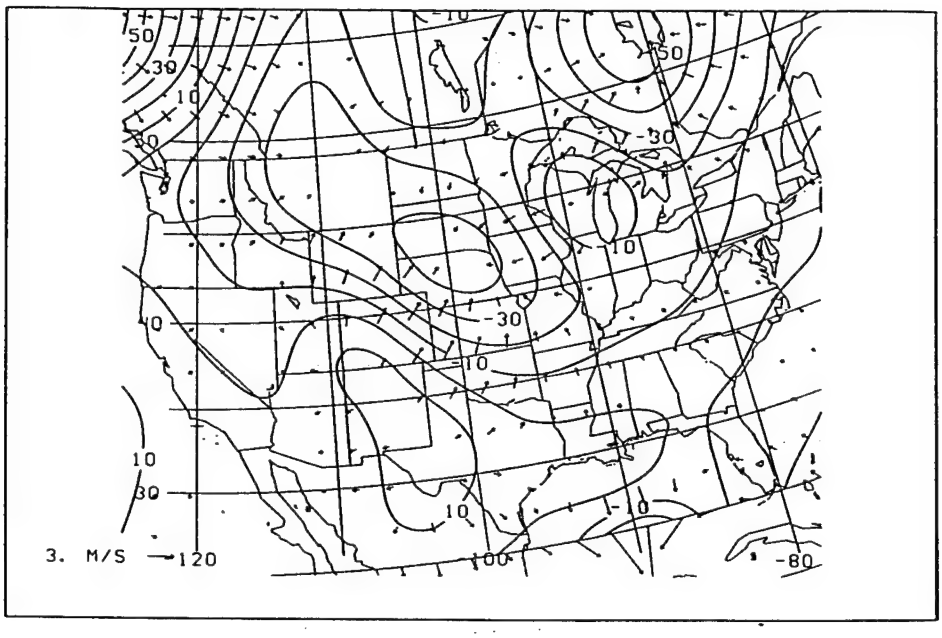

Figure 42. Same as in Figure 41 except for 0000 UTC, 18 October 1994.

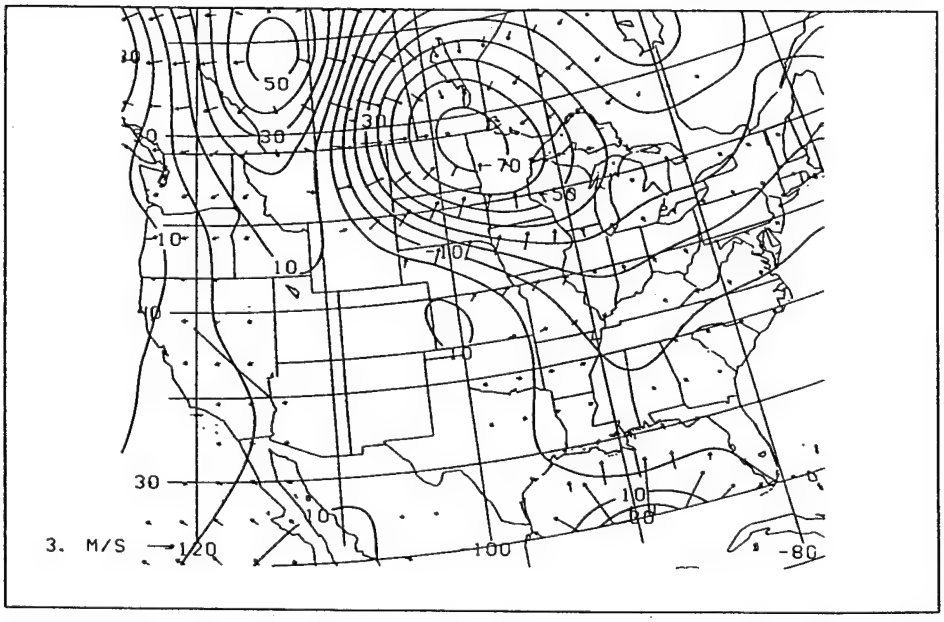

Figure 43. Same as in Figure 41 except for 1200 UTC, 18 October 1994.

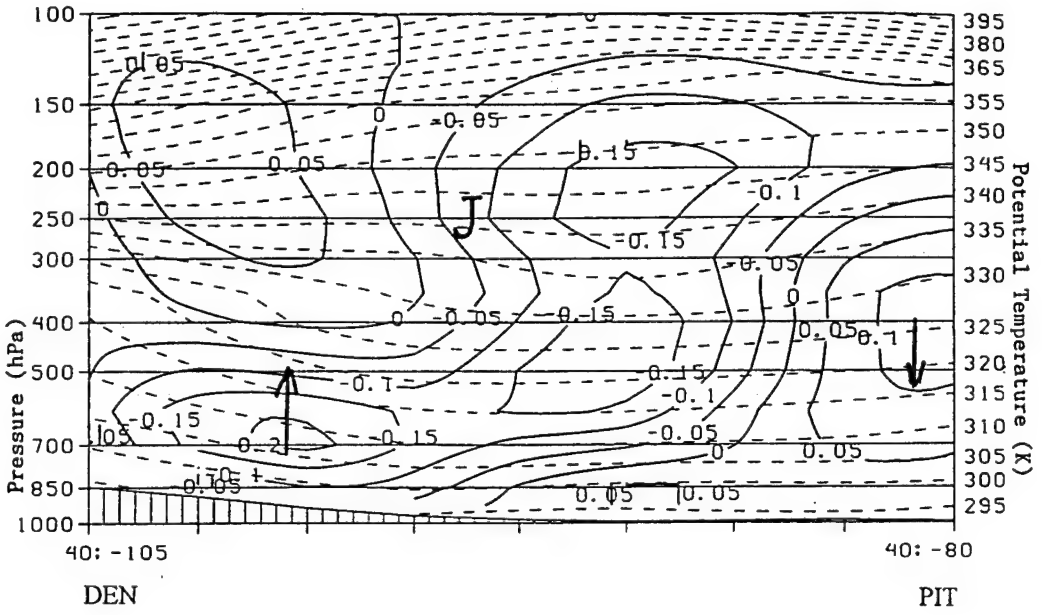

Figure 44. Vertical section showing vertical velocity (solid, Pa s^{-1}) and potential temperature (dashed, K) for 0000 UTC, 18 October 1994. J represents the position of the Polar Front Jet. The arrows indicate the direction of the vertical motion.

jet streak over the central United States. This time was chosen since it was during this time that the cyclone over the central United States was undergoing rapid deepening and intensification. The plot of the vertical velocity (ω=dp/dt) shows that there was rising motion on the order of 0.20 Pa s^{-1} in the cold air with sinking motion of 0.10 Pa s^{-1} in the warm air. Figure 45 is a cross-section of the component of the ageostrophic wind tangent to the cross-section plane. This cross-section shows that, in the lower troposphere, there was a component of the ageostrophic wind directed to the left with a magnitude of 4 to 8 m s^{-1}, while in the upper troposphere, the component was directed to the right of the jet streak. The LLJ appeared to occur in the return branch of the indirect circulation found in the exit region of the ULJ indicating that the two jets are coupled.

2. Low-level ageostrophic wind

Analysis of the vertical motion in the lower-levels of the atmosphere is accomplished by using Q-vectors. Sanders and Hoskins (1990) state that in a Q-vector analysis, the convergence of Q-vectors indicates upward vertical motion. They state that if the synoptic system is deep enough to fill the troposphere, then the Q-vector shows the direction of the ageostrophic motion in the lower troposphere. Hoskins et al. (1978) and Hoskins and Pedder (1980) give an in-depth review of the theory and a derivation of the Q-vector equation. Using the following definition:

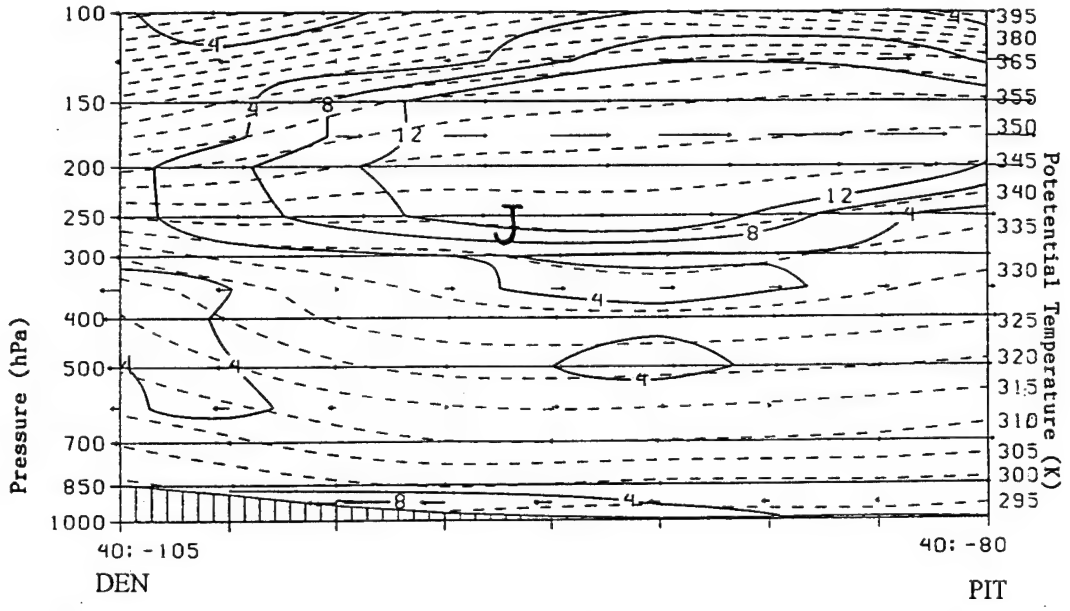

Figure 45. Vertical section showing the ageostrophic wind (m s^{-1}) component tangent to the plane of the section and potential temperature (dashed, K) at 0000 UTC, 18 October 1994. J represents the position of the Polar Front Jet.

$$Q_x = -(\partial u/\partial x \times \partial \theta/\partial x) + (\partial v/\partial x \times \partial \theta/\partial x) \quad (8)$$

$$Q_y = -(\partial u/\partial y \times \partial \theta/\partial y) + (\partial v/\partial y \times \partial \theta/\partial y) \quad (9)$$

where Q_x and Q_y are the x and y components of the Q vector, u and v are the x and y component of the wind, respectively, and θ is the potential temperature, the Q-vectors were determined. A review of the Q-vector field shows that at 1200 UTC 16 October (Fig. 46), Q-vector convergence was occurring over the area from northwest Texas into southern Nebraska. This is the area in which the lower-level baroclinic zone was located. By 0600 UTC 17 October, cyclogenesis was occurring over northwestern Texas, and an area of Q-vector convergence (Fig. 47) was located over the southeastern corner of Colorado into northwestern Texas. The LLJ had a jet streak of 18 m s^{-1} over northwestern Texas at 1200 UTC 17 October (not shown), and subsequent plots showed the LLJ had a maximum in speed in the vicinity of the convergence of the Q-vector.

C. Conclusions

The LLJ in this case developed in response to large-scale forcing. Therefore, this LLJ was classified as a Type 1 LLJ. The fall of the 850 hPa surface was associated with an isallobaric component of the ageostrophic flow accelerating toward the isallohypsic minimum. The increase in the wind speed was related to these isallohypsic minima located in Nebraska at 0000 UTC 18 October 1994, and over western Minnesota at 1200 UTC 18

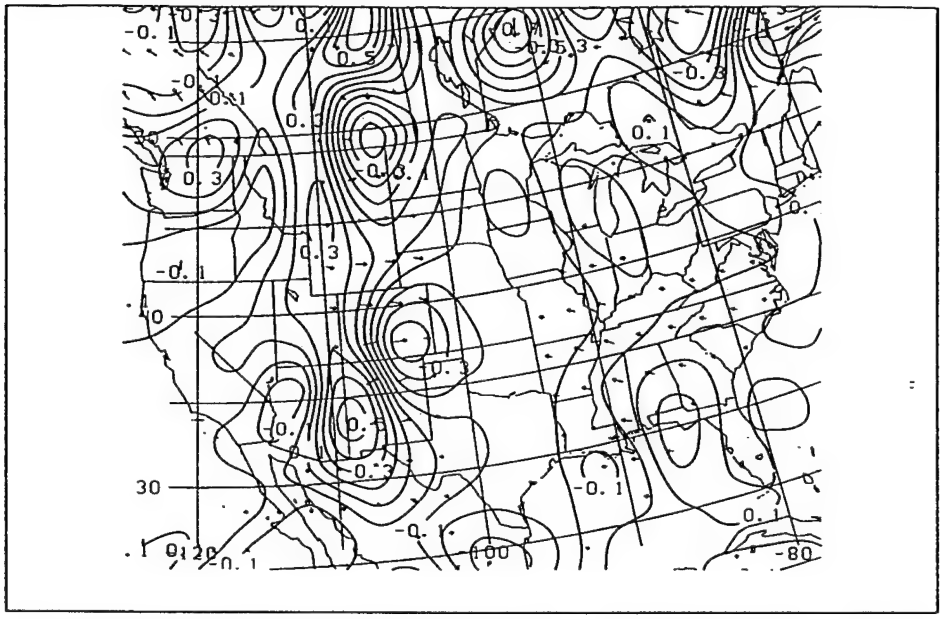

Figure 46. Plot of 850 hPa Q-vector divergence (solid, 10^{-15} K m^{-2} s^{-1}) and Q-vectors for 1200 UTC, 16 October 1994. The largest vector represents 4 x 10^{-10} K m^{-1} s^{-1}.

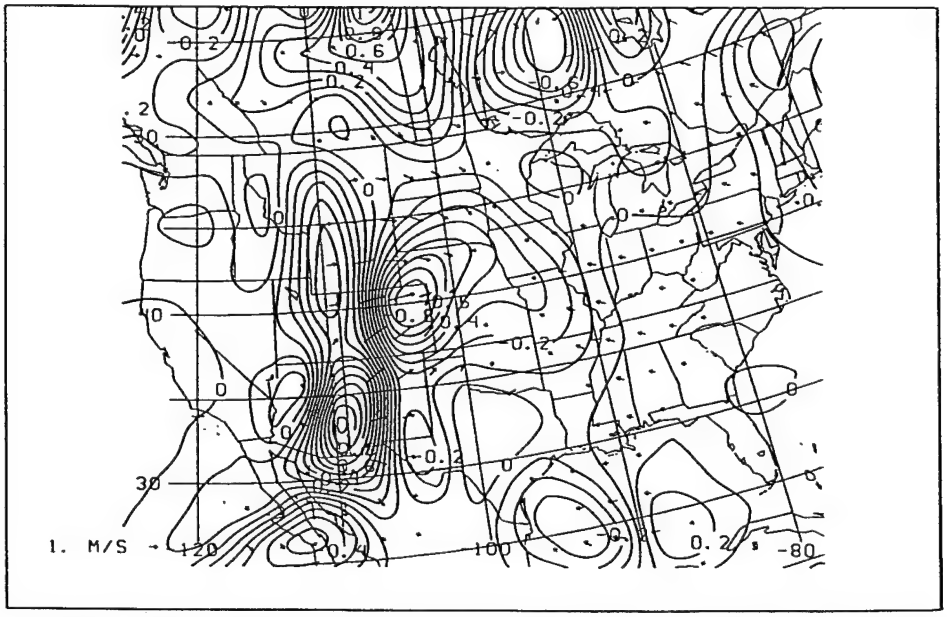

Figure 47. Same as in Figure 46 except for 0600 UTC, 17 October 1994. The largest vector represents 9 x 10^{-10} K m^{-1} s^{-1}.

October 1994.

The propagation of an upper-level jet streak into the region was related to the fall of the 850 hPa surface. The role of the upper-level jet was analyzed by examining the upper-level jet and the LLJ. The LLJ occurred in the return branch of the indirect circulation found in the exit region of the ULJ indicating that the two jets are coupled.

Analysis of Q-vectors was performed to study the ageostrophic wind in the lower atmosphere since the Q-vector can be used to show the direction of the vertical motion. In this case, the Q-vector analysis shows significant convergence and divergence at 850 hPa with the region of convergence of the Q-vectors occurring in the area of the LLJ and cyclogenesis. This indicated that the LLJ in this case may be driven by synoptic-scale forces associated with the upper-level cyclone which moves into the central United States.

CHAPTER VII

INTERACTION OF AN UPPER-LEVEL LOW, THE LOW-LEVEL JET, AND SURFACE CYCLOGENESIS: A CASE STUDY

Uccellini and Johnson (1979) show the interaction of the LLJ and the upper-level jet for a case associated with severe convection. This can be extended to the case where surface cyclogenesis is occurring. Examining 20 cases of LLJ formation during the cool season, Djurić and Damiani (1980) present an idealized model of the LLJ showing that the LLJ is a component of the flow associated with the surface cyclone.

Researchers from the 1940s into the 1980s have studied the development of upper-level cutoff cyclones and have shown that the formation of these lows is tied to the development of a fold in the tropopause. Air of stratospheric origin with high potential vorticity moves down the sloping isentropes leading to an intensification of these cyclones. As the high potential vorticity air becomes severed from the stratospheric reservoir and confined in the base of the cyclone, the cyclone cuts off from the flow. Advection of the potential vorticity maximum downstream of the cyclone results in the cyclone return to the basic westerly flow.

Hoskins et al. (1985) show that if an upper-level potential vorticity maximum moves over a region where there is a lower-level potential vorticity maximum, the formation of a surface cyclone is possible. Hoskins and Berrisford (1988) show this for the

case of the October 1987 storm which struck Great Britain. The case of 14-18 October 1994 showed similar characteristics to the October 1987 cyclone.

A. Mechanisms for Development

The development of the LLJ, upper-level cyclone and surface cyclogenesis are all interrelated. The development of the upper-level cutoff cyclone is related to the extrusion of potential vorticity from the stratosphere. A set of figures are presented here to describe a conceptual model of the atmospheric processes occurring in the cyclonic event of 16-18 October 1994.

The circulation that occurs around the jet stream is important in generating the fold in the tropopause related to the development of any upper cyclone. Figure 48 shows the tropopause fold and the circulation associated with the entrance region of the ULJ. The vertical motion in the entrance region of the jet stream results in a lowering of stratospheric air into the troposphere along the polar side of the jet. On the equatorial side of the jet, the vertical motion results in a lifting of the tropopause surface. This folding of the tropopause results in stable stratospheric air descending into the troposphere forming the upper-level frontal layer.

The stable air in the stratospheric region is characterized by a high potential vorticity value. For the case of 16-18 October, it was shown that air high in potential vorticity descended along the sloping isentropic surfaces in the upper-level frontal boundary

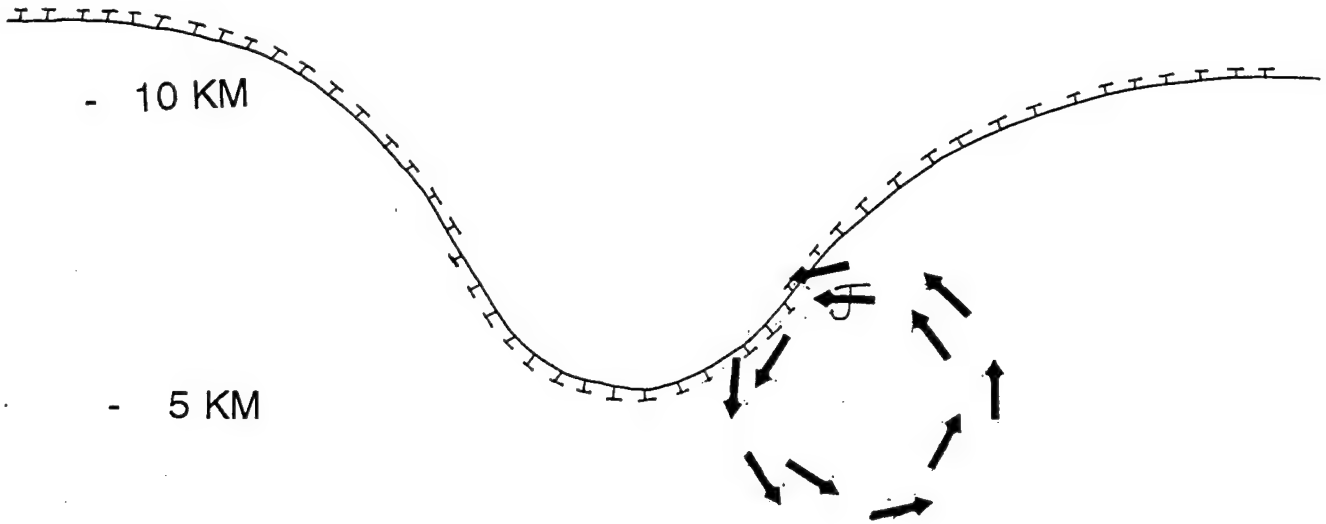

Figure 48. A schematic showing the folding of the tropopause in the vicinity of the jet stream. The arrows show the ageostrophic circulation with the T showing the direction of movement of the tropopause (Adapted from Djurić 1993).

to levels in the troposphere. These parcels conserved their potential vorticity during their descent. With the development of the stable frontal zone, the isentropes were tilted from the horizontal into the vertical reducing the static stability of this region. In order to conserve potential vorticity, the absolute vorticity increased providing additional spin for the upper-level cyclone.

At 0000 UTC 16 October as the upper-level low over the western United States was cutting off, a jet streak at 300 hPa was propagating into the central United States. At the same time, a trough was becoming established in the lee of the Rocky Mountains. With the fall in mean sea-level pressure over the lee of the Rockies and the tightening pressure gradient, a strong southerly flow developed over the central United States. This LLJ was associated with an increasing isallobaric component of the ageostrophic wind as the height of the 850 hPa surface fell in response to an approaching trough. The LLJ was coupled with the return branch of the indirect circulation found in the exit region of the upper-level jet. The LLJ transported warm air to the north helping to enhance the baroclinicity in the lee of the Rockies.

The upper-level cyclone became cut off from the flow as the potential vorticity maximum became separated from the stratospheric source and moved into the base of the cyclone. In some cases, cutoff cyclones are long-lived, but in this case the cut off nature of the cyclone was short-lived with the maximum of potential vorticity exported downstream of the cyclone and no additional potential vorticity being brought into the region of the cyclone.

The downstream movement of the potential vorticity maximum coincided with the observation of a lower-level potential vorticity maximum. This maximum near the 850 hPa level was situated in the region of a trough in the lee of the Rockies, and by 0600 UTC 17 October, the surface cyclone developed in this region. Figure 49 shows the development of a cyclone on the baroclinic zone in association with the fold in the tropopause as the upper-level potential vorticity maximum in the stratosphere aids in the development of a lower-level cyclonic circulation. The lower-level circulation with a southerly LLJ in the warm sector enhances the baroclinic zone as warm air is advected to the north and cold air to the south.

Between 0600 UTC and 1200 UTC 17 October, the pressure in the developing surface cyclone area fell at a rate of 0.33 hPa h^{-1}. The cyclonic circulation which formed did not extend deeply into the atmosphere. Figure 50 shows the developing cyclone with the lower-level front extending into the troposphere and the upper-level front extending downward. As the lower-level cyclonic circulation increases, the parcels in the lower atmosphere ascend into the middle troposphere along the isentropic surfaces.

The deepening rate of the cyclone increased significantly to 1 hPa h^{-1} after 1200 UTC 17 October when the polar jet/trough system associated with the upper-level cyclone moved into the Central Plains. Figure 51 shows the LLJ ascending in the warm air turning anticyclonically in the cold air ahead of the warm front. The ULJ is descending with the LLJ embedded in the return branch of the indirect circulation at the exit region of the ULJ. The enhanced circulation in the lower troposphere is enhancing the circulation in the upper

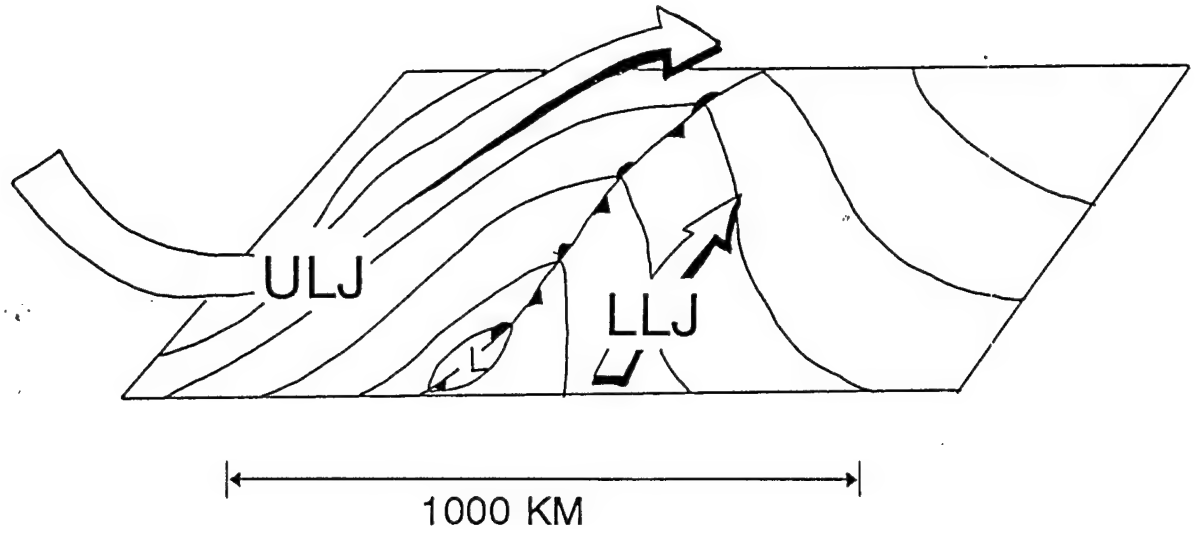

Figure 49. A schematic representation of cyclogenesis associated with the arrival of an upper-level cyclone and its associated maximum in potential vorticity over the lower-level baroclinic zone. The cores of the LLJ and ULJ are indicated by the double arrows.

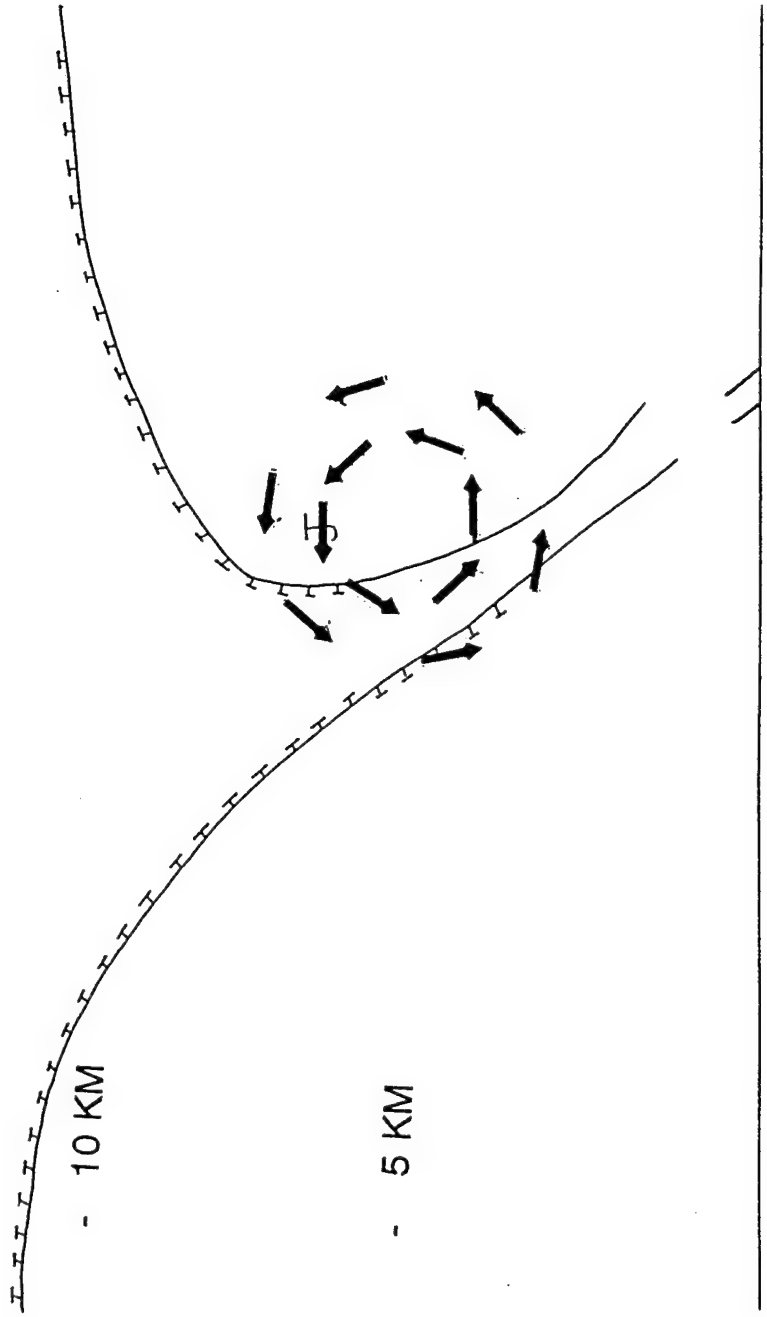

Figure 50. A schematic representation of cyclogenesis with the downward development of the upper-level front and the upward development of the lower-level front.

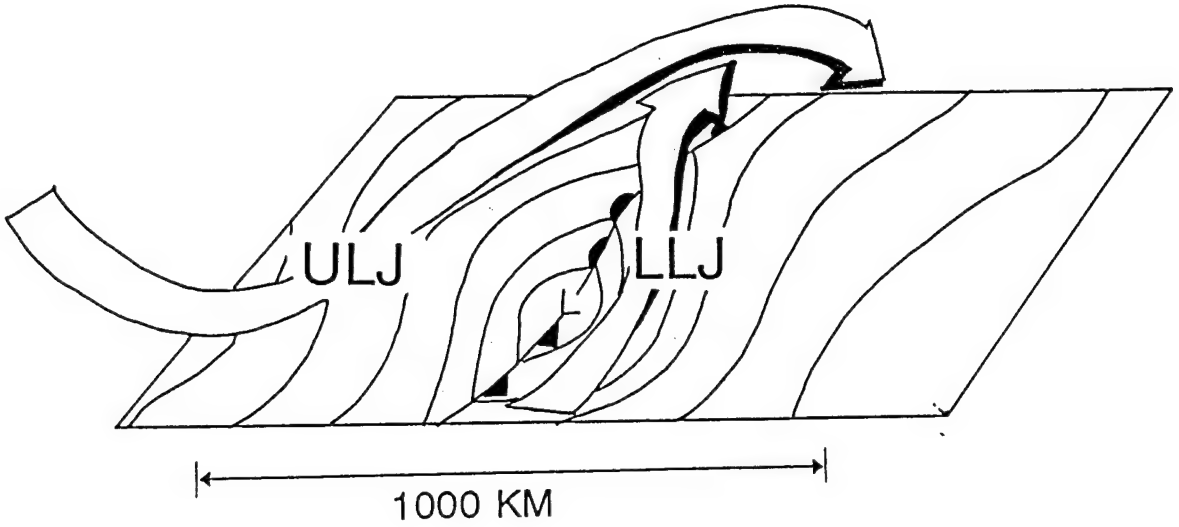

Figure 51. A schematic representation of the mature stage of cyclogenesis. The lower-level cyclone is deepening as the upper-level circulation is enhancing the lower-level circulation The LLJ is ascending in the warm air and turning anticyclonically as it ascends.

troposphere with the upper-level and lower-level fronts merging and assuming the appropriate position in the lower tropospheric cyclone (see Fig. 52). Figure 53 shows the at the occlusion phase of the lower level cyclone as the ULJ and LLJ interact with the mutual intensification of the upper and lower level circulations.

B. Conclusions

There is not one process which can be individually isolated which led to the development of the surface cyclone. The upper-level jet streak and upper-level cyclone were interrelated to the development of the LLJ and the surface cyclone with the LLJ coupled to the ULJ. The downward movement of air high in potential vorticity, and its interaction with a lower-level baroclinic zone appeared to enhance the lower-level circulation as the upper-level jet/trough system moved into a favorable position in the active region of the trough-ridge system. The rapid development of the surface cyclone appeared to be associated with the upward development of the lower-level cyclone and its associated front and the downward development of the upper-level front. Interaction of the upper-level cyclone and lower-level cyclonic circulation resulted in a mutual intensification of the cyclone circulation.

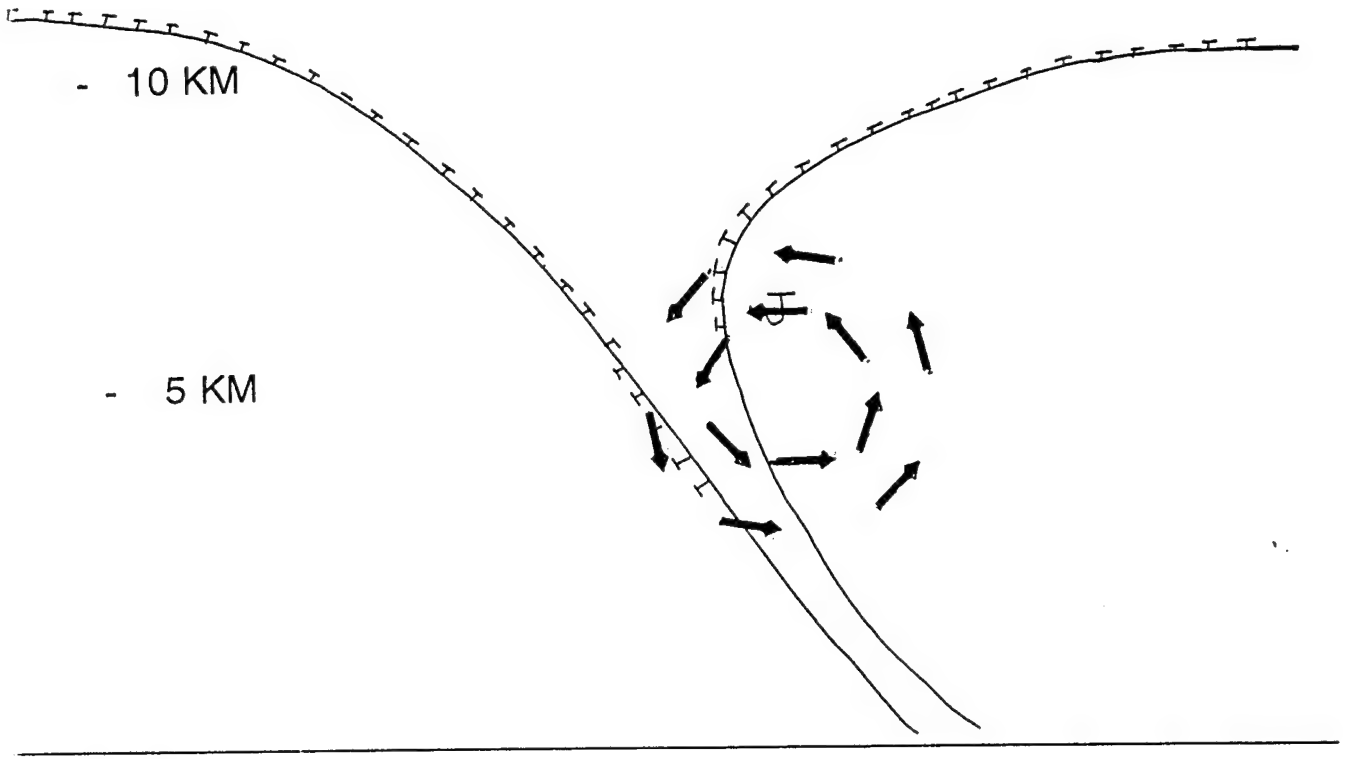

Figure 52. A schematic representation of the occlusion stage of cyclogenesis with the upper-level front and lower-level front merging and assuming the appropriate position in the cyclone.

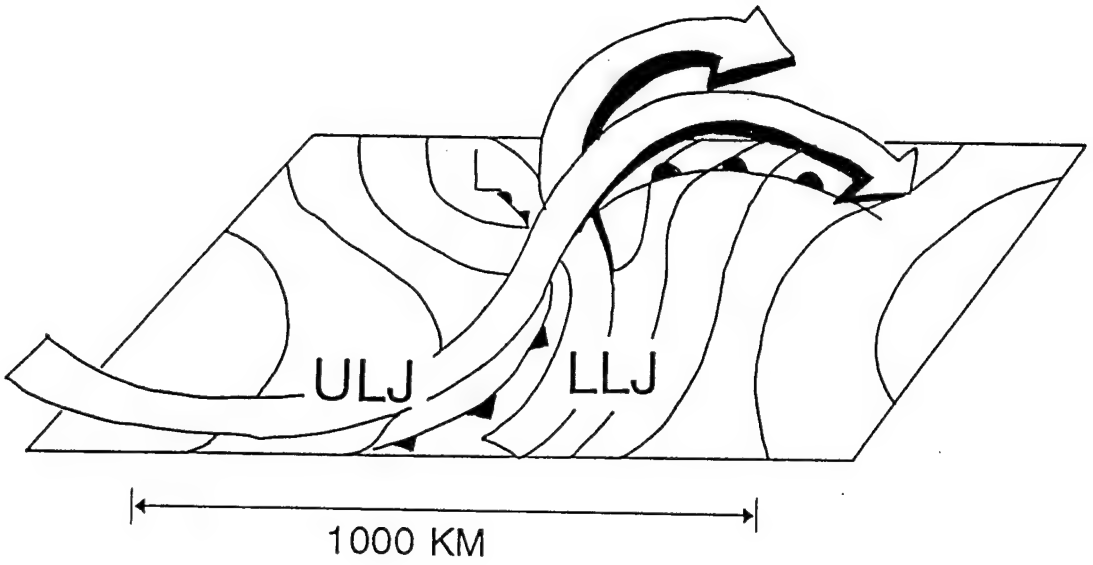

Figure 53. A schematic representation of the occlusion stage of cyclogenesis. The lower-level cyclone is occluded with the LLJ turning anticyclonically in the cold air. The upper-level jet is descending into the lower-level cyclone, and ascending as it approaches the downstream ridge.

CHAPTER VIII

SUMMARY AND DISCUSSION

The development and evolution of a cutoff cyclone during the period 16-18 October 1994 was examined. In conjunction with this cutoff cyclone, the LLJ and a surface cyclone were studied. A set of mechanisms using existing theories was proposed for the development and interaction of these three meteorological features. Results from the Eta Model were used to examine these features in a region which is sparse in data.

A. Summary of Conclusions

The following main points emerged from this research:

1. Upper-level cutoff cyclogenesis began as high potential vorticity air in the stratosphere descended into the troposphere in the vicinity of a tropopause fold. Separation of the maximum of potential vorticity from the stratospheric reservoir process and the isolation of the maximum in the base of the trough indicated that the cyclone was cut off from the westerly current. Following downstream advection of the potential vorticity maximum, the upper-level cyclone began to move to the east-northeast.

2. Surface cyclogenesis commenced about 12 hours after the arrival of the upper-level potential vorticity maximum over a lower-level potential vorticity maximum.

The rapid cyclogenesis phase began after the two potential vorticity anomalies interacted. It appears that the upper-level cyclone and lower-level cyclone interacted and a potential vorticity tower developed during the period of rapid deepening. The pressure fell by 15 hPa in 15 hours during this period.

3. The LLJ developed in response to large scale forcing. Analysis of the forces which lead to the development of the LLJ in this case show that this LLJ develops in association with the isallobaric acceleration at 850 hPa.

4. A vertical section through the exit region of the ULJ indicated that the LLJ was coupled to the ULJ in the return branch of the indirect circulation.

5. Q-vectors analysis shows that for this situation there is convergence in the vicinity of the LLJ at 850 hPa. This indicated that the LLJ in this case may be driven by synoptic-scale forces associated with the upper-level cyclone and jet streak which moves into the central United States.

6. There is a strong relationship between the upper-level cyclone, LLJ and surface cyclone in this case. Interaction of the three processes resulted in the development of a strong surface cyclone. The interaction of the upper- and lower-level potential vorticity maxima appeared to be associated with cyclogenesis. Rapid deepening and intensification occurred as the polar jet/ trough system moves into the active region of the trough-ridge system.

7. The LLJ through the advection of warm air enhanced the surface baroclinic zone and served as the warm conveyor belt in the cyclone. Parcels in the lower

troposphere ascended to higher levels carrying their potential vorticity to interact with the parcels descending from the upper troposphere.

B. Discussion of Research

The development and evolution of an upper-level cyclone was studied as it cut off over the southwestern United States. Bell and Bosart (1993) indicate that the formation of the cutoff cyclone begins when the potential vorticity maximum moves into the base of the trough. Separation of the potential vorticity maximum from its stratospheric reservoir and isolation of this maximum in the base of the trough initiates the cutting off process in this case. The downstream advection of the maximum results in the cutoff cyclone returning to the westerly current. The development of a lower-level potential vorticity anomaly and subsequent formation of a surface cyclone were related to this upper-level cyclone.

The presence of upper-tropospheric forcing was important in this case for the development of the LLJ. The development of the LLJ in this case was accompanied by the formation of a trough in the lee of the Rocky Mountains and cyclogenesis in southwestern Texas. The pressure gradient enhanced the development of the LLJ with the LLJ appearing in response to synoptic-scale forcing. The LLJ was coupled to the upper-level jet in the return branch of the indirect circulation in exit region of the upper-level jet.

The formation of the upper-level cyclone with an associated upper-level jet streak,

a LLJ, and a surface cyclone were all interrelated. The jet streak provided the circulation which resulted in the descent of air with high values of potential vorticity. The isolation of this high potential vorticity air in the base of a trough triggered the formation of a cutoff low. The downstream propagation of the potential vorticity maximum and its interaction with a lower-level maximum played a role in the development of a surface cyclone. The interaction of the upper-level maximum and lower-level anomaly in combination with the movement of the trough/polar jet system to the active region of the trough aided in the rapid development of a deep cyclonic circulation which extended into the upper troposphere.

REFERENCES

Barnes, S. L., and B. R. Colman, 1993: Quasi-geostrophic diagnosis of cyclogenesis associated with a cutoff extratropical cyclone: The Christmas 1987 storm. *Mon. Wea. Rev.*, **121**, 1613-1634

Beckman, S. K., 1973: A study of wind-speed maxima near the surface over the south-central United States. M. S. Thesis, Department of Meteorology, Texas A&M University, 73 pp.

Bell, G. D., and L. F. Bosart, 1993: A case study of the formation of an upper-level cutoff cyclonic circulation over the eastern United States. *Mon. Wea. Rev.*, **121**, 1635-1655.

Betts, A. K., 1986: A new convective adjustment scheme. Part I: Observational and theoretical basis. *Quart. J. Roy. Meteor. Soc.*, **112**, 677-691.

———, and M. J. Miller, 1986: A new convective adjustment scheme. Part II: Single column tests using GATE wave, BOMEX and arctic air-mass data sets. *Quart. J. Roy. Meteor. Soc.*, **112**, 693-709.

Black, T. L., 1988: The step-mountain, eta coordinate regional model: A documentation. NOAA/NWS/NMC, 47 pp [Available from the Development Division, W/NMC2, WWB, Room 204, Washington DC 20233.]

———, 1994: The new NMC mesoscale eta model: Descriptions and forecast examples, *Wea. Forecasting*, **9**, 265-278.

——, D. G. Deaven, and G. DiMego, 1993: The step-mountain eta coordinate model: 80 km 'early' version and objective verification. Technical Procedures Bulletin 412, NOAA/NWS, 31 pp. [Available from the National Weather Service, Office of Meteorology, 1325 East-West Highway, Silver Spring, MD 20910.]

Blackadar, A. K., 1957: Boundary layer wind maxima and their significance for the growth of nocturnal inversions. *Bull. Amer. Meteor. Soc.*, **38**, 283-290.

Bonner, W. D., 1965: Statistical and kinematic properties of the low-level jet stream. Res. Pap. 38, Satellite and Mesometeorology Project, University of Chicago, 54 pp.

DiMego, G., 1988: The NMC regional analysis system. *Mon. Wea. Rev.*, **116**, 977-1000.

Djurić, D., 1981: A numerical model of the formation and evolution of a low-level jet. *Mon. Wea. Rev.*, **109**, 384-390.

——, 1994: *Weather Analysis*, Prentice-Hall, 304 pp.

——, and M. S. Damiani, Jr., 1980: On the formation of the low-level jet over Texas. *Mon. Wea. Rev.*, **108**, 1854-1865.

——, and D. S. Ladwig, 1983: Southerly low-level jet in the winter cyclones of the southwestern Great Plains. *Mon. Wea. Rev.*, **111**, 2275-2281.

Hoecker, W. H., Jr., 1963: Three southerly low-level jet systems delineated by the weather bureau special PIBAL network of 1961. *Mon. Wea. Rev.*, **91**, 573-581.

Huschke, R. E., (ed.), 1970: *Glossary of Meteorology*, Amer. Meteor. Soc., 638 pp.

Holton, J. R., 1967: The diurnal boundary layer wind oscillation above sloping terrain. *Tellus*, **19**, 199-205.

Hoskins, B. J., and P. Berrisford, 1988: A potential vorticity perspective of the storm of 15-16 October 1987. *Weather,* **43**, 122-129.

———, and M. A. Pedder, 1980: The diagnosis of middle latitude synoptic development. *Quart. J. Roy. Meteor. Soc.*, **106**, 707-719.

———, I. Dragici, and H. C. Davies, 1978: A new look at the omega-equation. *Quart. J. Roy. Meteor. Soc.*, **104**, 31-38.

———, M. E. McIntyre, and A. W. Robertson, 1985: On the use and significance of isentropic potential vorticity maps. *Quart. J. Meteor. Soc.*, **111**, 877-946.

Janjić, Z. I., 1990: The step-mountain coordinate: Physical package. *Mon. Wea. Rev.* **118**, 1429-1443.

———, 1994: The step-mountain eta coordinate model: Further development of the convection, viscous sublayer, and turbulence closure schemes. *Mon. Wea. Rev.*, **122**, 927-945.

Kanamitsu, M., 1989: Description of the NMC Global Data Assimilation and Forecast System. *Wea. Forecasting*, **4**, 335-342.

Keyser, D., 1986: Atmospheric fronts: An observational perspective. *Mesoscale Meteorology and Forecasting*. Amer. Meteor. Soc. 216-258.

Kleinschmidt, E., 1950a: Über Aufbau und Entstehung von Zylonen (1.Teil). *Met Runds.* **3**, 1-6.

———, 1950b: Über Aufbau und Entstehung von Zylonen (1.Teil). *Met Runds.* **3**, 54-61.

Mesinger, F., 1984: The sigma system problem. *Preprints: Seventh Conf. on Numerical Weather Prediction,* Montreal, Amer. Meteor. Soc., 340-347.

———, Z. I. Janjić, S. Ničković, D. Gavrilov, and D. G. Deaven, 1988: The step-mountain coordinate: Model description and performance for cases of alpine lee cyclogenesis and for a case of an Appalachian redevelopment. *Mon. Wea. Rev.*, **116**, 1493-1518.

Ott, L., 1992: *An Introduction to Statistical Methods and Data Analysis*, Duxbury Press, 1051 pp.

Palmén, E., 1949: On the origin and structure of high-level cyclones south of the maximum westerlies. *Tellus*, **1**, 22-31.

———, and C. W. Newton, 1969: *Atmospheric Circulation Systems*. Academic Press, 603 pp.

Peltonen, T., 1963: A case study of an intense upper cyclone over eastern and northern Europe in November 1959. *Geophysica* (Helsinki), **8**, 225-251.

Petterssen, S. 1956: *Weather Analysis and Forecasting Vol 1, Motion and Motion Systems. 2nd ed.* McGraw Hill, 428 pp.

———, and S. J. Smebye, 1971: On the development of extratropical cyclones. *Quart. J. Roy. Meteor. Soc.*, **97**, 457-482.

Reed, R. J., 1955: A study of a characteristic type of upper-level frontogenesis. *J. Meteor.* **12**, 226-237.

———, and E. F. Danielsen, 1959: Fronts in the vicinity of the tropopause. *Arch. Meteor. Geophys. Bioklim*, **A11**, 1-17.

Sanders, F. and J. R. Gyakum, 1980: Synoptic-dynamic climatology of the "bomb". *Mon. Wea. Rev.*, **108**, 1589-1606.

———,and B. J. Hoskins, 1990: An easy method for estimation of Q-vectors from weather maps. *Wea. Forecasting*, **5**, 346-353.

Shapiro, M. A., 1978: Further evidence of the mesoscale and turbulent structure of upper-level jet stream-frontal systems. *Mon. Wea. Rev.*, **106**, 1100-1111.

Thorpe, A. J., 1985: Diagnosis of balanced vortex structure using potential vorticity. *J. Atmos. Sci.*, **42**, 397-406.

———, 1986: Synoptic-scale disturbances with circular symmetry. *Mon. Wea. Rev.*, **114**, 1384-1389.

Tollerud, E. I., K. W. Howard, and X-P. Zhong, 1991: Jet streaks and their relationship to heavy precipitation in Colorado front range winter storms. *Preprints, First International Symp. on Winter Storms*, New Orleans, Amer. Meteor. Soc., 97-100.

Uccellini, L. W., 1980: On the role of upper-tropospheric jet streaks and low-level jets in the Great Plains. *Mon. Wea. Rev.*, **108**, 682-703.

———, and D. R. Johnson, 1979: The coupling of upper and lower tropospheric jet streams and implications for the development of severe convective storms. *Mon. Wea. Rev.*, **107**, 682-703.

———, D. Keyser, K. F. Brill, C. H. Wash, 1985: Presidents' Day cyclone of 18-19 February 1979: Influence of upstream trough amplification and associated tropopause folding on rapid cyclogenesis. *Mon. Wea. Rev.*, **112**, 962-988.

——, P. J. Kocin, R. A. Petersen, C. H. Wash, and K. F. Brill, 1984: The Presidents' Day cyclone 18-19 February 1979: Synoptic overview and analysis of the subtropical jet streak influencing the pre-cyclogenetic period. *Mon. Wea. Rev.*, **112**, 31-55

——, R. A. Petersen, K. F. Brill, P. J. Kocin, and J. J, Tucillo, 1987: Synergistic interactions between an upper-level jet streak and diabatic process that influence the development of the low-level jet and a secondary coastal cyclone. *Mon. Wea. Rev.*, **115**, 2227-2261.

Weismueller, J. L., 1984: A plunging type 500-mb low. Central Region Tech Attach. 84-4, 4 pp. [Available from National Weather Service Central Region Headquarters, Scientific Services Division, Kansas City, MO 64106.]

Wexler, H., 1961: A boundary layer interpretation of the low-level jet. *Tellus*, **13**, 368-378.

VITA

Richard Lee Ritz was born in Fort Bragg, North Carolina on 7 June 1960 to Lt Col. and Mrs. Karl C. Ritz. He graduated from Sanderson High School, Raleigh, North Carolina in 1978. In 1985, he received a B.S. degree in Zoology and a B.S. degree in Meteorology from North Carolina State University. In 1988 he joined the United States Air Force.

He was stationed at Fort Riley, Kansas from 1988 to 1990 where he was the Assistant Staff Weather Officer and Tactical Weather Team Officer. He was stationed at Camp Casey, Republic of Korea from 1990 to 1991 where he was the Division Weather Officer. From 1991 to 1993, he was the Chief of the Weather Support Unit, Headquarters Air Force Special Operations Command, Hurlburt Field, Florida. Beginning August 1993, he was assigned to Texas A&M University under the Air Force Institute of Technology.

The author's permanent mailing address is:

4516 Gates Street

Raleigh, North Carolina 27609